

Sl. No.	<p style="text-align: center;">IIT Ropar List of Recent Publications with Abstract Coverage: June, 2024</p>
A	<p style="text-align: center;">Book(s)</p>
1.	<p>Donor-acceptor cyclopropanes in organic synthesis A Biju, P Banerjee - Book, ISBN: 9783527349876, Wiley, 2024</p> <p>Abstract: Facilitate milder, simpler reactions in organic synthesis with this cutting-edge family of building blocks Donor-Acceptor Cyclopropanes, or DACs, have attracted a resurgence of interest from organic chemists in recent decades for their role in facilitating various reactions such as cycloadditions, annulations, ring-opening and enantioselective transformations. The structural arrangement of DACs leads to milder, simpler reaction conditions, which have made them indispensable for a range of fundamentally and industrially important processes. Donor-Acceptor Cyclopropanes in Organic Synthesis covers comprehensively the chemistry and applications of this compound class. The result is an invaluable guide for any researcher looking to bring DACs to bear in their own areas of research or development. Readers will also find: A brief introduction of the history and reactivity of DACs Detailed discussion of reactions including Lewis acid-catalyzed cycloadditions, metal-free activation, asymmetric transformations, organocatalysis, and many more Application of DACs in natural product synthesis and pharmaceutical/agrochemical research Donor-Acceptor Cyclopropanes in Organic Synthesis is ideal for organic chemists, experts in catalysis, pharmaceutical researchers, and any other scientists interested in facilitating milder, simpler reactions.</p>
B	<p style="text-align: center;">Book Chapter(s)</p>
2.	<p>A review on fundamentals of cold spray additive manufacturing G Vinay, R Kant, H Singh - Modern Materials and Manufacturing Techniques: Book Chapter, 2024</p> <p>Abstract: The quest for decreasing the wastage during the production has paved the way for the invention of additive manufacturing (AM), however due to the melting of particles AM may not be suitable for all types of materials and repairing of any part is beyond the capability of current AM systems. On the other hand, cold spray, which started as a coating technique, has the ability to repair parts by depositing several mm layer thickness deposits without melting the feedstock. This feature makes it applicable to use as a coating/repair technique to deposit all types of metals. By employing the right thickness building strategy, one can build a complete part, which makes it a “manufacturing at need” kind of AM process where any part/repair can be done onsite. Since the process involves no melting, there is no need for combustibles/harmful gasses and there is no wastage of material. These features make cold spray additive manufacturing (CSAM) a sustainable and eco-friendly process. Through this chapter readers will be introduced to the history of cold spray, bonding mechanism, effect of process parameters and the post-processing involved in cold spray followed by strategies to make CSAM into a smart manufacturing system.</p>
3.	<p>An insight into applications of laser in modern era R Nair, R Kant, H Gurung - Modern Materials and Manufacturing Techniques: Book Chapter, 2024</p> <p>Abstract: In the era of advanced manufacturing, development in technology is increasing at a fast rate, but at the same time modern industries are also focusing on sustainable and economical</p>

	<p>manufacturing approaches. Laser is one such technology that has been attracting researchers and industries over decades for various manufacturing and research purposes. In the 21st century, laser has expanded its utilization in almost every field, from daily usage to aerospace applications. The efficiency of lasers helped industries to evolve rapidly and fulfil high customer demands. Laser technology opened many doors for researchers to get better insight into materials and their behaviours. It has also helped the medical sector to evolve, where patients can now go through a painless and easy mode of treatment. This chapter focuses on the application of laser technology in the academic, industrial, defence and medical sectors.</p>
4.	<p>An overview of robot assisted additive manufacturing S Rathor, A Kumar, R Kant, E Singla - Modern Materials and Manufacturing Techniques: Book Chapter, 2024</p> <p>Abstract: This chapter focuses on the use of robotic systems in the manufacturing industry, specifically in the field of additive manufacturing. In today's competitive manufacturing environment, productivity, flexibility, and agility are key elements. Multiple degrees of freedom robots are showing promise in automating manufacturing processes. The discussion in this chapter highlights how the use of robots in additive manufacturing is experiencing significant growth due to their ability to achieve higher precision and efficiency. The chapter covers the major additive manufacturing processes that can be enhanced with advanced robotic systems and explores the potential of using robotic systems with advanced materials. This chapter also explores recent advancements in industrial applications and future perspectives, considering the integration of robots with additive manufacturing processes. To illustrate the concepts discussed, the chapter presents a few examples of robotic additive manufacturing systems.</p>
5.	<p>Gasification and combined heat and power (CHP) from lignin Subhashini, M Jeremias, VS Sikarwar - Lignin Chemistry: Characterization, Isolation, and Valorization: Book Chapter, 2024</p> <p>Abstract: The search for renewable energy sources has provided a new prominence to biomass to meet the increasing energy demand worldwide. Although the energy conversion of biomass is an ancient art, recently there has been an upsurge in thermochemical conversion of biomass. Biomass gasification is a widely used thermochemical process for obtaining products with more value and potential applications than the raw material itself. This chapter starts with a discussion on the cardinal composition of wood (cellulose, hemicellulose, and lignin). It is followed by an insightful consideration of the various sources of lignin, their composition, characterization, availability, and different conventional methods of treating lignin to obtain from their sources. Light is shed on the gasification process of different lignins and the combined potential for heat and power. It also involves an investigation of various process parameters and descriptions, product distributions, applications of obtained products along with advantages and limitations of the lignin gasification process.</p>
6.	<p>Green composites for sustainable applications P Bhowmik, R Kant, H Singh - Modern Materials and Manufacturing Techniques: Book Chapter, 2024</p> <p>Abstract: Environmental pollution has become an unavoidable problem nowadays, and plastic disposables play a vital role in polluting the earth's surface and water bodies. In a recent discovery, it has been found that plastic molecules were present in the water sample collected from the deepest part of the ocean where even human intervention hasn't been made. To reduce plastic pollution, researchers are developing biodegradable counterparts of plastic disposables. Biocomposites play a vital role in solving many of these existing problems with an eco-friendly approach. This chapter will elaborate on the sustainable approach to developing biocomposites with natural fibres and epoxy or resins. The study focuses on dividing natural fibres into their</p>

	<p>subcategories of plant-based fibres and animal fibres and studying their advantages and disadvantages in developing biocomposites. It also includes studies related to naturally available epoxy and resin, which can be a sustainable alternative to the commercially available synthetic counterparts.</p>
7.	<p>Machine learning and additive manufacturing: A case study for quality control and monitoring A Pratap, A Pandey, N Sardana - Modern Materials and Manufacturing Techniques: Book Chapter, 2024</p> <p>Abstract: Integrating machine learning algorithms with additive manufacturing has significant potential to enhance the quality control process in the revolution of Industry 4.0. As additive manufacturing becomes increasingly prevalent in the manufacturing industry, the need for quality control has become more critical than ever. In this competitive era, identifying patterns and trends of large volumes of generated data during the additive manufacturing process is very difficult or sometimes impossible for human beings; therefore, deep learning algorithms can be an effective and efficient tool to determine and analyze the trend of such a large amount of data in additive manufacturing. This can help find potential defects at its initial stage, improve quality, and reduce manual inspection costs. In addition, deep learning algorithms can help to optimize the additive manufacturing process, thus proving it cost-effective and efficient. By analyzing data from sensors monitoring the printing process, deep learning algorithms can identify patterns and optimize process parameters, leading to improved print quality and consistency, reduced waste, and minimized risk of defects. Machine learning algorithms in quality control and process optimization can significantly enhance the overall efficiency and productivity of the manufacturing process in Industry 4.0. With the ability to rapidly analyze vast amounts of data, deep learning algorithms can detect subtle defects and help manufacturers identify opportunities for improvement in the additive manufacturing process. In this chapter, various case studies have been used to demonstrate that the effective utilization of deep learning in the field of additive manufacturing and quality control can help manufacturers to improve product quality, reduce waste, and optimize the manufacturing process, making them more competitive, effective, and efficient in the age of Industry 4.0.</p>
8.	<p>Machining performance and optimization of process parameters of monel alloy 400 using ECM process PS Rao, A Sinha...R Kant... - Modern Materials and Manufacturing Techniques: Book Chapter, 2024</p> <p>Abstract: Monel alloy 400, a mixture of copper and nickel, is widely renowned for its resistance to chemicals and physical strength. This alloy is most likely among the toughest as well as least corrosive metal recognized in the industry and research fields. These qualities have increased its uses in a variety of domains such as aerospace, marine, and automotive. Because work hardens fast on its surface, Monel alloys are very difficult to cut using typical machine equipment or other procedures. The current study examines the effect of ECM method parameters like applied voltage source (V), electrolyte concentration (EC) and inter electrode gap (IEG) upon material removal rate (MRR), tool wear rate (TWR), and surface roughness (Ra). The basic electrolytes utilized in machining of Monel Alloy 400 are a mixture of aqueous sodium nitrate (NaNO₃) and sodium chloride (NaCl). As an experimental strategy, the Box–Behnken design (BBD) generated from response surface methodology (RSM) is utilized, and the effects of variables and their relationships are investigated and process variables adjusted.</p>
9.	<p>Materials technology and its advancements involving nanotechnology, hydrogels, and its impact assessment on various aspects of improving the healthcare system S Ghosh, P Yadav, B Das - Industrial Microbiology and Biotechnology: An Insight into Current Trends: Book Chapter, 2024</p>

	<p>Abstract: In recent years, materials technology has experienced remarkable progress, especially in the fields of nanotechnology and hydrogels. Nanotechnology, which allows for precise manipulation of materials at the nanoscale, has brought significant enhancements to hydrogels. By incorporating nanoparticles into hydrogel structures, their mechanical strength, water absorption capacity, structural integrity, drug-loading capabilities, and targeting abilities have all been greatly improved. The emergence of nanocomposite hydrogels has ushered in new dimensions in the healthcare sector. These advanced materials possess tunable mechanical properties, antimicrobial activities, cytotoxicity, and optical features, making them highly versatile and beneficial for various medical applications. Their ability to match the mechanical properties of specific tissues and organs has made hydrogels invaluable in tissue engineering and regenerative medicine, where tailored support for cellular growth and tissue repair is crucial. The seamless integration of hydrogels with living tissues has also led to reduced adverse reactions in biological environments, facilitating the development of biocompatible implants, wound dressings, and tissue regeneration scaffolds. This chapter focuses on the fundamental characteristics of hydrogels and delves into the numerous advancements in their material properties, which have been achieved through innovative synthesis techniques and nanoengineering approaches. Furthermore, the chapter highlights the role of nanotechnology-enabled hydrogels which has led to the development of nanosensors, injectable hydrogels, and nanostructure-coated medical devices and implants that enhance biocompatibility and integration. Moreover, it discusses the promising potential for personalized medicine through the fusion of nanotechnology and hydrogels. By tailoring hydrogels with nanoscale components personalized to individual patient needs, treatments can be optimized based on genetic profiles, resulting in more effective outcomes, and minimized adverse effects.</p>
10.	<p>Nanoparticle-laden flow for solar absorption V Khullar, S Soni, H Tyagi - Handbook of Multiphase Flow Science and Technology: Book Chapter, 2023</p> <p>Abstract: Nanoparticle-laden fluid (or more popularly “nanofluid”) could be engineered to efficiently absorb as well as transport solar energy. This flow involves suspension of nano-sized particles (particle size <100 nm) within a fluid. The fluid may be in gaseous or liquid state depending on the application or a naturally occurring phenomenon. Nanoparticles of various materials, shapes, and sizes can be suspended within a fluid, without agglomeration, through certain chemicals known as surfactants or capping agents. Such nanoparticle-laden fluids can be prepared in situ through chemical methods, or these can be obtained by mixing the solid nanoparticles to a fluid. There are advantages of using nano-sized particles as compared to micro-sized particles. Nanoparticle-laden flows do not lead to clogging of the fluid passage or other components like pumps and valves. Moreover, the fact that the optical properties of metallic and semiconductor nanoparticles are dependent on their shape, size, and the surrounding dielectric media makes them easily usable for engineering highly solar selective nanoparticle dispersions at very low volume fractions. This chapter describes in detail the mechanism of absorption of solar energy by volumetric absorption solar thermal systems employing nanoparticle-laden fluid flows. Thermophysical, rheological, and optical properties of the nanoparticle-laden fluids have been explored. Critical analysis of the previous studies relevant to nanofluid-based solar thermal systems reveals that these novel solar thermal systems hold huge potential and warrant further exploration for practical realization of such novel solar thermal systems.</p>
11.	<p>Reactivity of cyclopropyl monocarbonyls P Kumar, IM Taily, P Singh, P Banerjee - Donor Acceptor Cyclopropanes in Organic Synthesis: Book Chapter, 2024</p>

	<p>Abstract: Donor–acceptor cyclopropane (DAC) having one carbonyl group has emerged as an interesting molecule with diverse reactivity lines as compared to the classical DACs with a diester group as the acceptor. In addition to the inherent property of being a three-carbon dipolar species for a formal (3 + n) cycloaddition process, these cyclopropane monocarbonyls (aldehyde and ketones) also provide the option of involving the carbonyl group directly in the transformation rather than just being an activator of the cyclopropane carbon–carbon bond between the donor and the acceptor groups. It is also quite fascinating to see how these comparatively less activated cyclopropanes undergo C–C bond cleavage without demanding any particularly harsh reaction conditions. In this Chapter, first the unique reactivity of donor–acceptor cyclopropyl carbonyls will be discussed, followed by the general synthetic strategies for their synthesis. Later in the chapter, the application of these molecules in various ring-opening/ring-opening-cyclization processes will be discussed, which will finally be followed by the discussion on the utilization of cyclopropane monocarbonyls in the total synthesis of biologically important molecules.</p>
12.	<p>Use of nanoparticles in the healthcare industry for antimicrobial effects M Sharma, S Hazra, B Das - Industrial Microbiology and Biotechnology: An Insight into Current Trends; Book Chapter, 2024</p> <p>Abstract: Due to the inappropriate and overuse of antibiotics in different sectors, such as healthcare systems, food processing units, and dairy farms, in the past few decades, antibiotic resistance has arisen as a major threat to humankind as well as to animals. Superbugs like Enterobacteriaceae sp., Staphylococcus sp., Pseudomonas sp., Acinetobacter, and E. coli show broad-spectrum antibiotic resistance and cause millions of deaths per year. By 2050, there are predictions of ten million deaths per year due to infection by multidrug-resistant microbes. Over a few decades, the introduction of nanosystems and their application in healthcare and the development of healthcare products have given nanobiotechnology an edge over conventional antibiotics and healthcare products. Nanobiotechnology is a branch of science that works on the combined principle of nanotechnology and molecular biology. Broadly divided into five major classes of metal, ceramics, lipids, polymeric, and semiconductor nanoparticles, these nanostructures have applications in various healthcare sectors including gene therapy, drug delivery, cardiac and brain disease treatment, cancer diagnosis and treatment, treatment of genetic disorders, CNS disorders treatment, and much more. This chapter provides details on various nanoparticles and their mode of action. The diagnostic and therapeutic applications of nanobiotechnology in the healthcare industry as well as in industrial use along with prospects of undergoing advancements in this field can help in the development of potential healthcare-based products. Here, we also discussed the recent scientific research on antimicrobial–antifungal–antiviral activity, antibiofilm activity, anticancer activity, drug delivery systems, and food technology systems to establish the potential of nano-systems in the advancement of healthcare and industrial sector.</p>
13.	<p>Utilization of ultrasonic vibration and laser energies during sustainable machining N Deswal, R Kant - Modern Materials and Manufacturing Techniques: Book Chapter, 2024</p> <p>Abstract: Manufacturing operations are the major contributor to the development of any product or part; however, these manufacturing industries are also major sources of pollution. Machining processes are vital processes to be used in industries and they consume a significant amount of natural resources and energies globally. Moreover, the usage of cutting fluids not only enhances the production cost but also negatively impacts the machining operator and environment. Consequently, sustainable manufacturing has become a global priority in response to environmental challenges and the depletion of natural resources. Various efforts have been made during the machining process to minimize those challenges such as dry machining, minimum quantity lubrication (MQL), cryogenic machining, and hybrid machining processes. Among all these advancements, hybrid machining processes have gained significant importance due to the</p>

	utilization of various energies during the machining process. Ultrasonic vibration and thermal energies are the most commonly utilized energies during the machining process. Utilization of these energies has shown improved machining performance during the machining process, especially without using any cutting fluids. Additionally, both ultrasonic vibration and thermal energies have also been utilized simultaneously during the machining performance, and improved machining performance has been obtained compared to conventional machining process.
C	Conference Proceeding(s)
14.	<p>Energy and exergy optimization of a double-stage Kalina cycle with a bottoming Goswami cycle A Singh, R Das - 9th Thermal and Fluid Engineering Conference (TFEC), 2024</p> <p>Abstract: The main emphasis of this study is the idea of enhancing the standalone double-stage Kalina cycle's working performance by employing a bottoming cycle to recover its low-grade exhaust heat. The literature search indicates that using the absorption refrigeration cycle, the Goswami cycle, or the organic Rankine cycle are all viable options for the above goal. In this context, the previous research on the utilization of the Goswami cycle was limited to recovering heat from the Kalina cycle's turbine exhaust, leaving unexplored the possibility of using the heat from its ammonia-weak solution. Moreover, the Kalina-Goswami cycle's previous configuration constrained its operation to a single ammonia concentration, which restricted the assembly's ability to recover heat in different thermal contexts. The present combined scheme uses two recuperators for heat recovery from both turbine exhaust and ammonia-weak solution of the double-stage Kalina cycle. Additionally, separate absorbers are used for the topping and the bottoming cycles so as to ensure concentration independence between them. The comparative analysis shows that the heat recuperation helps the combined scheme to produce higher exergy of product with fewer exergy losses and that too when it is running at concentration lower than that of the standalone Kalina cycle. Optimization techniques are used to examine the combined scheme's ability to adjust in various thermal circumstances. Under ideal working conditions, the combined scheme generated 7.88 kW more turbine work, 4.27 kW of auxiliary sensible cooling, dissipated 5.59 kW less exergy and is 1.09 time more exergy-efficient than the standalone Kalina cycle.</p>
15.	<p>Experimental study on photocatalytic efficiency of TiO₂-coated cement plaster in reduction of ambient TVOC S Mishra, P Haldar, I Dadha - Proceedings of the 7th International Conference on Geotechnics, Civil Engineering and Structures (CIGOS- 2024), 2024</p> <p>Abstract: The emission of pollutants and harmful gases like VOCs from vehicles and industries have degraded the air quality significantly and consequently affected human and structural health. Although the photo-catalysis technique is widely used for the treatment of air pollution, selecting an efficient photo-catalyst having strong oxidizing ability and chemical stability is still a major challenge. In this paper, an attempt has been made to investigate the photocatalytic efficiency of TiO₂ in reducing air pollutants such as total VOCs. A parametric study has been conducted with the characterization of different proportions of TiO₂ sprayed over the selected building surface to determine the optimum dose. The decontamination efficacy of TiO₂ was obtained from the initial and final concentration of known TVOCs inside the reaction chambers. The obtained results showed the variation of degradation rate from 7E-07 to 5E-07 s-1cm-2 of coating and the maximum degradation rate constant of 8.70E-06 s-1cm-2 corresponding to 14.9% of TiO₂ dose by cement weight. Which justifies the viability of TiO₂ in the purification of the surrounding environment and advocates its widespread use on the building surfaces.</p>
16.	Integration of biomass gasification with a gas turbine cycle and a triple-pressure cogeneration cycle

	<p>A Singh, R Das - 9th Thermal and Fluid Engineering Conference (TFEC), 2024</p> <p>Abstract: An integrated system is presented that produces and burns syngas completely into fluegas, and then uses the latter as a thermal input in a triple-pressure cogeneration cycle after first being used in a gas turbine cycle. The study focuses on monitoring the outputs under parameters that are supposed to change frequently while the system is running in a near-real working environment. The primary variables that fluctuate are the temperature of syngas during gasification (T_{syn}), the moisture content of biomass (MC), the temperature of fluegas after combustion (T_{flue}), and the concentration of ammonia in the cogeneration cycle (x_{NH3}). It has been shown that an increment in the T_{syn} and the MC leads to a decrease in the work output of the gas turbine cycle, while on the other hand, they increase the work and cooling outputs of the cogeneration cycle. Also, an increase in x_{NH3} benefits the cogeneration cycle's work and cooling production capacity while having no influence on the turbine cycle's work output. However, the rise in T_{flue} creates contradictory/conflicting conditions in the gas turbine cycle and the cogeneration cycle, causing their outputs to fluctuate when the system is in function. Based on the above results, it is seen the maximums of the outputs from both cycles occur at the same T_{flue} and x_{NH3}, however, the maximums of their respective cycles come at different T_{syn} and MC. The maximum recorded output from the gas turbine cycle and the cogeneration cycle are 12699.49 kW, 1106.16 kW and 833.73 kW, respectively.</p>
17.	<p>Net-zero assessment of solar energy-driven absorptionradiant air conditioning system G Singh, R Das - 9th Thermal and Fluid Engineering Conference (TFEC), 2024</p> <p>Abstract: Radiant cooling unit (RCU) is one of the most promising technologies towards energy efficient buildings. Integrating low-grade thermal energy driven absorption cooler (AC) with the RCU is becoming an attractive alternative to the compression cooler (CC) based RCU. The present study aims to investigate the performance of AC driven RCU for achieving the net-zero energy building status target using the EnergyPlus simulation tool. In particular, AC-coupled RCU and the CC-driven ventilation unit (VU) are considered for the building's air conditioning. The considered building dimensions are 50 m × 33 m and have a total 4950 m² of floor area, approximately. Here, the electricity requirement of the building for lighting, cooling, equipment, etc., is accomplished by installing solar photovoltaic (PV) on the roof. Moreover, a loop of solar thermal collector (500 m²) is installed to fulfill the heating requirement of AC. An auxiliary heating element is also provided with a solar collector loop to address any solar energy intermittency. In order to evaluate the net zero energy target of the building, simulations are done for different installed areas of solar PV (varying between 500 m² - 800 m²) under the weather conditions of composite climate. Simulation results reveal that the target of net-zero building under considered solar PV area is 31.8% - 50.9%. It is also observed that, as solar PV installation area increases, the net energy demand decreases due to the shading effect, and even with the maximum installation of solar PV, fully gridindependent/ complete net-zero building cannot be ensured.</p>
18.	<p>Package power delivery architecture for high performance computing systems with a 1 kW IVR operated in CCM-DCM boundary mode condition RR Khorasani, X Li, JW Kim, P Murali, R Sharma... - 2024 IEEE 74th Electronic Components and Technology Conference (ECTC), 2024</p> <p>Abstract: This paper investigates a package power delivery architecture for high-performance computing (HPC), incorporating a novel modular multi-phase integrated voltage regulator (IVR). The 1-kW 48-12/1 V architecture integrates an efficient interleaved buck-derived converter at the continuous-discontinuous boundary condition, facilitating parallel-connected networks of embedded inductors to deliver hundreds of amperes per phase. Due to the increased duty cycle and zero switching losses provided for the high side switch, the converter's frequency can be further increased up to 50 MHz with 8 parallel phases and 100 MHz with 16 parallel phases for a</p>

	<p>48/1 V, 1 kW architecture. A conceptual 3-D stacked architecture using stacked glass substrates with flip chip GaN switches and embedded inductors, and capacitors is presented, offering a high-density single-stage 48-12/1 V IVR for the next generation of data center applications.</p>
<p>19.</p>	<p>Performance projection of stacked silicon nanosheet-FET architectures for future technology node A Goel, A Rawat, B Rawat - International Workshop on the Physics of Semiconductor and Devices (IWPSD, 2021), 2024</p> <p>Abstract: Silicon-based gate all around nanosheet field-effect transistor (NS-FET) have been emerged as a promising candidate for 5 nm and beyond technology node as it offers superior gate control over the channel and excellent current drivability. Despite stacked nanosheet designs have been reported the excellent switching performance over Fin-FET at the 3 nm technology node, their performance at lower technology node is limited by carrier mobility degradation and layer parasitic capacitance. Therefore, this work examines and compares the emerging nanosheet stacking architectures, such as stacked, sub-stacked, and tree-type, for logic applications at 1 nm technology node. The performance analysis of NS-FET, is done using a fully calibrated three-dimensional (3-D) TCAD simulation, based on self-consistent solutions of 3-D Poisson's equation and Boltzmann equation with correction terms for accounting the short channel device physics. The results show that, at 1 nm technology node, tree-FET architecture with three channels is a more favorable candidate over stacked and sub-stacked stacking architectures with higher ON current, lower device delay, and smaller power delay product. The tree-type nanosheet stacking architecture offers several performance benefits and is expected to be a promising architecture for future low-power digital applications.</p>
<p>20.</p>	<p>Solar energy integration in direct contact membrane distillation for clean water production J Dwivedi, KS Chauhan, H Tyagi - 9th Thermal and Fluid Engineering Conference (TFEC), 2024</p> <p>Abstract: Due to population growth and pollution, the demand for pure water has increased steadily over the years. As membrane distillation operates primarily with low-grade heat, it may be a viable solution to the problem. This paper examines the integration of direct-contact membrane distillation integration with solar collectors to generate clean water. Using mathematical modeling and numerical simulation, the optimal operating conditions for Direct contact membrane distillation under varying solar irradiance flux conditions are determined. Heat transport mechanism, mass transport mechanism, and fluid flow behavior are analyzed using the effectiveness-NTU method. The most important system parameter, mass flux is evaluated for different cities of India throughout the year, the flow behavior for low and high solar flux. It is recommended to operate the system under a laminar regime during periods of low-temperature gradient, i.e., low solar irradiance, particularly in the morning and evening. However, when there is a high-temperature gradient, i.e., a high solar irradiance flux, it is recommended to operate the system under a turbulent regime, particularly at midday. It is observed that when the flow changes from laminar to turbulent flow there is an increase of 7 to 18% in mass flux has been observed.</p>
<p>21.</p>	<p>Vertical power delivery for high performance computing systems with buck-derived regulators S Krishnakumar, M Choi, RR Khorasani, R Sharma... - 2024 IEEE 74th Electronic Components and Technology Conference (ECTC), 2024</p> <p>Abstract: With traditional power delivery architectures in state-of-the-art high-power (>1 kW) high-current density systems (>1 A/mm²), over 30% of the system-wide power is dissipated within the power delivery system, i.e., during the delivery of power from a printed circuit board (PCB) to functional die(s). Historically, in high-power systems, efficient low-power density voltage regulators have been placed on PCB, to minimize the conversion loss and advanced</p>

	<p>low-resistance interconnect technologies have been utilized to reduce the lateral routing loss in packaging power distribution network (PPDN). While power loss is reduced linearly with lower PPDN resistance, current reduction is desired due to the quadratic dependence of power on current. To efficiently deliver current from PCB to functional die, distributed vertical power delivery (DVDP) is preferred in this work. With this approach, power is delivered horizontally at high-voltage low-current and converted to low-voltage high-current close to functional die, near points-of-load (POLs), with optimal number of compact, power-efficient distributed on/in-interposer voltage regulators (VRs). Thus, lateral distribution of VRs is promising for mitigating conduction loss in both the VRs and horizontal packaging interconnect components. To increase the conversion efficiency and current density, an advanced network of parallel-connected vertically-stacked inductors and Gallium Nitride (GaN) power devices are considered. Analytical loss models and model-guided design methodology for optimizing the PCB-to-POL loss in a DVDP system are proposed in this work. A preferred power architecture for delivering 1-kW power to a functional 500-mm² die is determined based on the proposed models and methodology, exhibiting system-wide efficiency of 85.6% and power density of 2 W/mm².</p>
D	Journal Article(s)
22.	<p>2D–3D heterostructure of PtS_{2-x}/Ga₂O₃ and their band alignment studies for high performance and broadband photodetector G Bassi, D Kaur, R Dahiya, M Kumar - Nanotechnology, 2024</p> <p>Abstract: For deep ultraviolet (UV-C) photodetectors, gallium oxide (Ga₂O₃) is a suitable candidate owing to its intrinsic ultra-wide band gap and high stability. However, its detection is limited within the UV-C region, which restricts it to cover a broad range, especially in visible and near-infrared (NIR) region. Therefore, constructing a heterostructure of Ga₂O₃ with an appropriate material having a narrow band gap is a worthwhile approach to compensate for it. In this category, PtS₂ group-10 transitional metal dichalcogenide stands at the top owing to its narrow band gap (0.25–1.65 eV), high mobility, and stability for heterostructure synthesis. Moreover, heterostructure with Ga₂O₃ sensing in UV and PtS₂ broad response in visible and IR range can broaden the spectrum from UV to NIR and to build broadband photodetector. In this work, we fabricated a 2D–3D PtS_{2-x}/Ga₂O₃ heterostructure based broadband photodetector with detection from UV-C to NIR region. In addition, the PtS_{2-x}/Ga₂O₃ device shows a high responsivity of 38.7 AW⁻¹ and detectivity of 4.8 × 10¹³ Jones under 1100 nm light illumination at 5 V bias. A fast response of 90 ms/86 ms illustrates the device's fast speed. An interface study between the PtS_{2-x} and Ga₂O₃ was conducted using x-ray photoelectron spectroscopy and ultraviolet photoelectron spectroscopy (UPS) which confirmed type-I band alignment. Finally, based on their band alignment study, a carrier transport mechanism was proposed at the interface. This work offers a new opportunity to fabricate large-area high-performance 2D–3D heterostructures based photodetectors for future optoelectronics devices.</p>
23.	<p>A hybrid effective medium description for nanoporous gold films and thickness-mediated control of optical absorption J Singh, NK Gupta, S Sarkar - Nanotechnology, 2024</p> <p>Abstract: With the increasing demand for sensing platforms operating across UV, visible, and near-infrared wavelengths, nanoporous gold has emerged as an ideal substrate for rapid, quantitative detection of analytes with excellent specificity and high sensitivity. This study investigates thickness-mediated compositional changes and their impact on scattering characteristics of thin nanoporous gold films fabricated using selective chemical etching. Specifically, we observe thickness-induced morphological and structural changes across different fabricated samples from 25-100nm in thickness. Upon their optical characterization across UV-VIS-NIR spectral regime, we notice that the constitutional differences among samples</p>

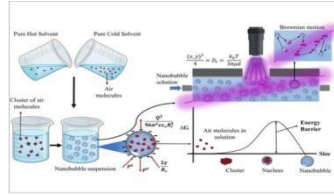
	<p>manifest distinctively & deterministically in their total optical scattering response. In order to gain insights into these observed scattering responses and to fathom the subtle connections between structural properties of NPG films and their optical response, a hybrid theoretical model comprising Maxwell-Garnett & Bruggeman effective medium approximations has been adopted. Our approach not only allows to appropriately account for the inhomogeneous nature of these films, but also corroborates well with the atomic force microscopy characterizations of the fabricated samples. Furthermore, tracing such a theoretical model is important as it helps in systematically ascertaining additional loss terms emerging in the complex dielectric function of films due to their nanoscale porosity & roughness, permitting a good reproduction of measured optical spectra. We believe, our approach will not only facilitate accurate regulation of losses in NPG thin films but will also aid in deriving customized optical performance from them, thereby advancing their potential applications in sensing and beyond.</p>
24.	<p>A novel selective harmonic mitigation PWM technique with THD minimization using second-order sliding modes P Kalkal, AVR Teja - IEEE Transactions on Industrial Electronics, 2024</p> <p>Abstract: This article proposes a novel selective harmonic mitigation technique based on higher order slidingmode control. The method aims to reduce total harmonic distortion (THD) while mitigating multiple harmonics as necessary according to existing standards, such as IEEE 519-2022. Unlike selective harmonic elimination (SHE), which can only eliminate a fixed number of harmonics, the proposed method can accommodate ($m - 1$) or more harmonics corresponding to m switching angles per quarter wave. The proposed methodology constrains the number of switching angles similar to SHE but achieves a lower THD and meets the IEEE 519-2022 requirements by alleviating multiple harmonics simultaneously. Complete details of the proposed algorithm are provided for a general case with m switching angles. Simulations in MATLAB/Simulink and experiments on a field-programmable gate array (FPGA) prototype validate the technique for $m = 5$ switching angles. Various test cases demonstrate the ability to mitigate specific harmonics while minimizing THD. Notably, the proposed SHM technique could mitigate up to four additional lower order harmonics above SHE with just five switching angles and two levels.</p>
25.	<p>A novel strategy to elicit enduring anti-morphine immunity and relief from addiction by targeting Acr1 protein nano vaccine through TLR-2 to dendritic cells S Nanda, MA Zafar, T Lamba, JA Malik, MA Khan... - International Journal of Biological Macromolecules, 2024</p> <p>Abstract: Morphine addiction poses a significant challenge to global healthcare. Current opioid substitution therapies, such as buprenorphine, naloxone and methadone are effective but often lead to dependence. Thus, exploring alternative treatments for opioid addiction is crucial. We have developed a novel vaccine that presents morphine and Pam3Cys (a TLR-2 agonist) on the surface of Acr1 nanoparticles. This vaccine has self-adjuvant properties and targets TLR-2 receptors on antigen-presenting cells, particularly dendritic cells. Our vaccination strategy promotes the proliferation and differentiation of morphine-specific B-cells and Acr1-reactive CD4 T-cells. Additionally, the vaccine elicited the production of high-affinity anti-morphine antibodies, effectively eliminating morphine from the bloodstream and brain in mice. It also reduced the expression of addiction-associated μ-opioid receptor and dopamine genes. The significant increase in memory CD4 T-cells and B-cells indicates the vaccine's ability to induce long-lasting immunity against morphine. This vaccine holds promise as a prophylactic measure against morphine addiction.</p>
26.	<p>A unified cyber attack detection and mitigation framework for an islanded ac microgrid S De, R Sodhi - IEEE Transactions on Systems, Man, and Cybernetics: Systems, 2024</p>

	<p>Abstract: This article proposes a novel three-step framework to accurately detect, estimate and mitigate cyber-attacks like unauthorized data manipulation and hijacking controller attacks which can jeopardize the entire frequency and voltage stability of an autonomous microgrid (MG). Step-1 proposes a novel maximum mean discrepancy (MMD)-based index to detect and locate the attacked distributed energy resources (DERs); in Step-2, an unknown input observer (UIO) is proposed to coarsely estimate the unknown false data injection attack (FDIA) parameters; and Step-3 develops a backstepping integrated sliding-mode control (BSMC) to compensate the attack by injecting reverse control input bias. The efficacy of the proposed cyber-attack detection and mitigation framework is rigorously tested under various types of cyber attacks on the modified IEEE-13 bus distribution test feeder operated in an islanded mode, modeled in RSCAD and is validated with real-time digital simulator (RTDS). The performance and superiority of the proposed detection scheme are compared with an existing method through hardware-in-the-loop (HIL) simulation control environment.</p>
27.	<p>Acemannan coated, cobalt-doped biphasic calcium phosphate nanoparticles for immunomodulation regulated bone regeneration D Negi, K Bhavya, D Pal, Y Singh - Biomaterials Science, 2024</p> <p>Abstract: Biomaterials are used as scaffolds in bone regeneration to facilitate the restoration of bone tissues. The local immune microenvironment affects bone repair but the role of immune response in biomaterial-facilitated osteogenesis has been largely overlooked and it presents a major knowledge gap in the field. Nanomaterials that can modulate M1 to M2 macrophage polarization and, thus, promote bone repair are known. This study investigates a novel approach to accelerate bone healing by using acemannan coated, cobalt-doped biphasic calcium phosphate nanoparticles to promote osteogenesis and modulate macrophage polarization to provide a prohealing microenvironment for bone regeneration. Different concentrations of cobalt were doped in biphasic calcium phosphate nanoparticles, which were further coated with acemannan polymer and characterized. The nanoparticles showed >90% cell viability and enhanced cell proliferation along with osteogenic differentiation as demonstrated by the enhanced alkaline phosphatase activity and osteogenic calcium deposition. The morphology of MC3T3-E1 cells remained unchanged even after treatment with nanoparticles. Acemannan coated nanoparticles were also able to decrease the expression of M1 markers, iNOS, and CD68 and enhance the expression of M2 markers, CD206, CD163, and Arg-1 as indicated by RT-qPCR, flow cytometry, and ICC studies. The findings show that acemannan coated nanoparticles can create a supportive immune milieu by inducing and promoting the release of osteogenic markers, and by causing a reduction in inflammatory markers, thus helping in efficient bone regeneration. As per our knowledge, this is the first study showing the combined effect of acemannan and cobalt for bone regeneration using immunomodulation. The work presents a novel approach for enhancing osteogenesis and macrophage polarization, thus, offering a potent strategy for effective bone regeneration.</p>
28.	<p>Advanced oxidation of Arsenic(III) to Arsenic(V) using ozone nanobubbles under high salinity P Koundle, GN Goud, N Gopinathan, N Nirmalkar - Journal of Environmental Chemical Engineering, 2024</p> <p>Abstract: Arsenic, a highly toxic element, is present in various water resources as As(III) and/or As(V). The removal of As(V) using adsorption is considered to be easier than the removal of As(III). In this work, we report the oxidation of As(III) to As(V) using ozone nanobubbles. Ozone has been widely used in the advanced oxidation process (AOP) to remove organics and inorganics in wastewater. The major advantage of ozone nanobubbles is their enhanced half-life, which leads to higher ozone solubility in water. In addition, the rate of mass transfer by using nanobubbles can be enhanced drastically. The effect of ozone flow rates, initial As(III) concentrations, pH levels, and the presence of salt is systematically studied in this work. The present results revealed that ozone nanobubbles positively impacted the oxidation of As(III) to</p>

	<p>As(V). AOP process based on O₃ NBs (nanobubbles) was most efficient with 99% oxidation rates of 1 ppm of As(III) within 20 minutes at 6.5 ppm ozone concentrations. An acidic pH of 3-7 promoted quick oxidation due to the high mass transfer coefficient of ozone nanobubbles. About ~70% degradation of As(III) to As(V) was achieved with 0.10854 min⁻¹ rate constant at acidic (pH = 3) compared to ~39% degradation with 0.046 min⁻¹ rate constant at pH =11. The presence of salt (~50 mM) in the solution not only hindered the ozone mass transfer coefficient but also reduced the stability of nanobubbles. The detection of reactive oxygen species, particularly hydroxyl radical was unravelled by utilizing 2-propanol as a scavenger.</p>
29.	<p><u>Advancing sustainable lignin valorisation: Utilizing Z-scheme photocatalysts for efficient hydrogenolysis of lignin's β-O-4, α-O-4, and 4-O-5 linkages under ambient conditions</u> R Ghalta, R Srivastava - Green Chemistry, 2024</p> <p>Abstract: Lignin, a crucial component of lignocellulosic biomass, holds immense promise for advancing biorefineries and producing sustainable energy alternatives. This study engineered a CN/rGO/BMO (2 : 1) heterojunction photocatalyst with varying Pd NP loading to selectively target the hydrogenolysis of challenging C–O ether bonds in lignin model compounds. Specific focus was on β-O-4, α-O-4, and the formidable 4-O-5 linkages. The 4-O-5 linkage, due to its high dissociation energy, poses a significant challenge. Electrochemical and spectral analyses unveiled improvements in charge separation, leading to delayed recombination of charge carriers in the heterojunction photocatalyst. Decorating the heterojunction with Pd NPs exhibited an elevated work function and a low Fermi energy level, facilitating the accommodation of photogenerated electrons and enabling efficient H₂ dissociation. Such enhancement facilitated the cleavage of all three linkages, including the resistant 4-O-5 bonds under ambient conditions. The photocatalyst exhibited effective cleavage, yielding aromatic (toluene, phenol, ethylbenzene) and aliphatic (cyclohexane, ethylcyclohexane) products. Selectivity modulation was achieved by adjusting the time, hydrogen pressure, and Pd loading. Furthermore, this photocatalytic approach successfully transformed simulated lignin bio-oil containing all three linkages into valuable monomers. The alcoholic solvents efficiently harnessed photogenerated holes and prevented electron–hole recombination. The photocatalyst also demonstrated the capability to produce monomers from the native lignin extracted from teak wood sawdust. Emphasizing the focus on the reaction pathway and mechanism, scavenging studies and analyses were conducted, including UPS and VBXPS, to establish the Z-scheme charge transfer mechanism within the heterojunction. These findings provide a sustainable and efficient pathway for lignin valorisation in biorefineries, significantly contributing to the advancement of green fuels and aligning with the principles of green chemistry.</p>
30.	<p><u>An optimized switching integrated transmitter pad for generating orthogonal H-field components to localize implanted devices</u> VK Srivastava, A Sharma - IEEE Journal of Electromagnetics, RF and Microwaves in Medicine and Biology, 2024</p> <p>Abstract: This paper proposes an optimized switching integrated transmitter to generate highly non-uniform magnetic field (H-field) components for near-field localization applications. The localization accuracy of a magnetic-based localization system depends on the degree of non-uniformity present in the H-field distribution. Targeting this, several state-of-the-art designs presented eight spatially distributed transmitter structures. However, the absence of required H-field components at several receiver positions resulted in poor localization performance. To overcome this problem, an overlapping coil transmitter structure has been proposed in this work that spreads the H-field components at the receiver region. Further optimization of the transmitter coil design parameters is performed analytically to accomplish a highly non-uniform H-field at the receiver location and miniaturize the transmitter size. A time-divisional approach has been exploited and realized using a switching technique to acquire the required voltage samples at the receiver. The proposed transmitter is realized using a high-frequency Litz wire, and the switching</p>

	<p>is performed by adopting DPDT switches. The fabricated prototype is experimentally verified, and the measured results show a good agreement with the analytical result. This demonstrates the potential of the proposed transmitter for near-field localization applications such as the localization of biomedical implants, wireless endoscopy capsules, etc.</p>
31.	<p>Analysis of stiffened in-homogeneous plates AK Pathak, SS Padhee - AIP Conference Proceedings, 2024</p> <p>Abstract: In the context of reinforcing a plate with a stiffener, the structure experiences a localized shift in the neutral plane. This shift occurs due to the geometric difference introduced by the stiffener. In this study, an analytical model for nonlinear analysis of stiffener reinforced plates is proposed. Instead of treating the stiffened plate as two separate structures (the stiffener and the plate), this model considers it as a single continuous structure with varying material properties in the thickness direction. To achieve this, the Variational Asymptotic Method (VAM) is employed which reduces the dimensions of the stiffened plate systematically while maintaining the desired level of accuracy. This approach takes advantage of the small thickness of the structure compared to its other dimensions. By breaking down the original 3-D elasticity problem into a through-the-thickness analysis and a geometrically nonlinear 2-D analysis, a closed-form solution for the through-the-thickness analysis is obtained. As a result of which a reduced dimensional (2D) model of the structure is created, which is further studied using the finite element method. In the present approach, the bottom plane of the structure is considered as the reference plane. The geometric discontinuity was taken into account during The dimensional reduction process. To validate the findings, the results obtained from the present study are compared with those obtained from a 3-D finite element analysis.</p>
32.	<p>Brønsted acid-catalyzed cascade ring-opening/cyclization of 3-ethoxy cyclobutanones to access 2,8-dioxabicyclo[3.3.1]nonane derivatives A Hazra, T Kanji, P Banerjee - The Journal of Organic Chemistry, 2024</p> <p>Abstract: A cascade ring opening of 3-ethoxy cyclobutanones followed by a double cyclization strategy has been developed via Brønsted acid catalysis. A range of 2,8-dioxabicyclo[3.3.1]nonanes are obtained from various substituted naphthols in a one-pot and open flux manner. Additionally, a 15-membered macrocycle has been synthesized by ring closing metathesis as a synthetic application.</p> <div style="text-align: center;"> <p> <ul style="list-style-type: none"> <li style="margin-right: 10px;">● Brønsted acid catalysis of cyclobutanone <li style="margin-right: 10px;">● Michael addition/cyclization <li style="margin-right: 10px;">● Macrocycle preparation <li style="margin-right: 10px;">● Metal free <li style="margin-right: 10px;">● Open flux <p>16 examples up to 85% yield</p> </p></div>
33.	<p>Bulk nanobubbles through gas supersaturation originated by hot and cold solvent mixing A Sharma, N Nirmalkar - Langmuir, 2024</p> <p>Abstract: The nucleation mechanism of bulk nanobubbles remains unclear despite the considerable attention they have received in recent years. We propose two hypotheses: (i) The gas supersaturation in the bulk liquid is the primary factor for nanobubble nucleation, and (ii) the mixing of the same solvent at varying gas solubilities should produce nanobubbles, provided that the first hypothesis is correct. To test this hypothesis, we performed extensive experiments on nanobubble nucleation in both water and organic solvents. The temperature difference between hot and cold samples ranged from 10 to 80 °C in pure solvents such as water, methanol, ethanol, propanol, and butanol prepared and mixed in equal proportions. To the best of our knowledge, we report bulk nanobubble nucleation by mixing hot and cold solvents for the first time. The refractive index value calculations using Mie scattering theory confirmed the existence of</p>

nanobubbles. When surface tension dominates over surface charge, the critical work for nanobubble formation is $\Delta F_c \propto 1/\xi^2$, and when surface charge dominates over surface tension, the critical work is $\Delta F_c \propto \xi^{1/4}$. Our experimental results verify such dependency by measuring nanobubbles nucleated with varying degrees of gas supersaturation.



[Compact polarization-insensitive microwave metamaterial absorber with hepta-band characteristics](#)

S Garg, P Jain...N Sardana... - Physica Scripta, 2024

34.

Abstract: This paper presents an ultra-thin and compact metamaterial absorber (MMA) capable of achieving near-perfect absorption peaks across the C, X, Ku, and K frequency bands. The MMA structure features a modified metallic plus-shaped resonator surrounded by symmetric L-shaped resonators within a compact size of $13 \times 13 \text{ mm}^2$. The absorber exhibits seven absorption peaks at different resonant frequencies including 4.23, 6.48, 10.62, 12.92, 14.03, 17.39, and 18.11 GHz. With a thickness of 0.0225λ and a compact size of 0.1833λ at the lowest frequency, the absorber offers remarkable thinness and compactness. Different characteristics of the absorber, such as normalized impedance, surface current distribution, and electric field distribution, are also examined. The polarization-insensitive behavior of the MMA is assessed through absorption and reflection responses under different polarization and incident angles. The Equivalent Circuit Model (ECM) of the metamaterial absorber is also designed to accurately represent the MMA unit cell across all resonant frequencies. Experimental validation of the proposed MMA confirms its performance consistency with simulation results. The proposed MMA design holds potential for applications in defense, detection, and sensing. The sensing ability of the MMA is analyzed using simulations at different refractive index values.

[Comprehensive assessment of PCM integrated roof for passive building design: A study in ergo-economics](#)

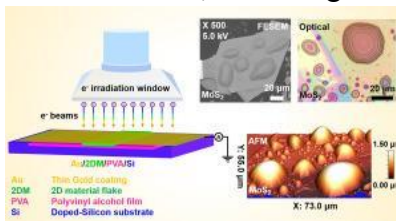
PJ Abass, S Muthulingam - Energy and Buildings, 2024

35.

Abstract: There has been a notable surge in energy demand within the building sector of developing nations, particularly in the context of space cooling and heating, which constitute significant portions of energy consumption. The thermal performance of a building's roof slab plays a crucial role in determining these heating and cooling requirements. To address this, the utilization of Phase Change Material (PCM) to enhance the building's thermal energy storage capacity has emerged as an innovative strategy for reducing energy demand. This study assesses the thermal behavior of a building envelope integrated with macroencapsulated PCM in a real subtropical environment. Experimental setups include both a conventional slab unit (Ref-SU) devoid of PCM and a PCM (OM37) integrated slab unit (Exp-SU). Analysis entails examining variations in temperature, heat flow, thermal loadings, and maximum heat gain reduction. Economic metrics, such as electricity savings, simple payback periods, and CO2 emissions savings, are also scrutinized. The investigation aims to elucidate the efficacy and underlying parameters governing the PCM's performance in reducing thermal loads in the Indian city of Rupnagar. Findings indicate that the Exp-SU configuration reduces indoor temperatures by $4.0 \text{ }^\circ\text{C}$ during sunny hours, resulting in 33.33 % more electricity savings for space cooling compared to heating, with a simple payback period of 5.7 years. Additionally, the heat flux in Exp-SU is reduced by 60.6 % compared to Ref-SU and thermal load by up to 49.8 %. Furthermore, Exp-SU achieves a 44.24 % reduction in CO2 emissions for space cooling compared to heating with a maximum heat gain reduction of 40.3 %.

36.	<p>Critical velocity for cold-sprayed coatings L Palodhi, PK Ray - Transactions of the Indian Institute of Metals, 2024</p> <p>Abstract: The cold-spray technology has been rapidly gaining in popularity, especially over the last two decades, due to its ability for depositing coatings at relatively low temperatures in contrast to other thermal spray methods. A key challenge for this technique lies in optimization of process parameters. Particle deposition occurs by plastic deformation of the particle and the substrate, which requires a high kinetic energy of impact. This calls for a minimum threshold velocity called the critical velocity and happens to be a key factor affecting process efficiency. In this review, we focus on numerical, theoretical and experimental approaches towards measuring the critical velocity (v_{cr}) and subsequently elucidate the factors affecting v_{cr}.</p>
37.	<p>Determination of frequency-dependent dynamic properties of rocks using the nonresonance method S Rohilla, R Sebastian - International Journal of Geomechanics, 2024</p> <p>Abstract: Assessing the dynamic properties of rocks remains a foundational pursuit in the field of rock engineering, providing crucial insights into their mechanical behaviors across a spectrum of loading conditions, including static, cyclic, and dynamic scenarios. This paper expounds upon the utilization of the nonresonance (NR) torsional shear test and its implications for understanding rock responses, particularly in the context of low and medium loading rates. The NR method serves as a pivotal tool for investigating model rock materials subjected to loading conditions characterized by low frequencies and amplitudes. Renowned for its efficacy, this method allows the simultaneous determination of two critical dynamic parameters: shear modulus (G) and damping ratio (D), all at a specific loading frequency. It has been ascertained that the loading rate increased as the loading frequency and applied amplitude of loading increased. With increasing loading rate, the shear modulus consequently increased while the damping ratio decreased. It is observed that the dynamic responses of both ramp and sinusoidal loading waveforms increase concurrently with the amplitudes of the applied torque and loading frequencies. The sinusoidal waveform exhibits greater dynamicity than the ramp waveform at a certain loading rate. Furthermore, this study delves into the intricate analysis of the nonlinear viscoelastic dynamic response exhibited by rocks, utilizing the modified hyperbolic (MH) model and the Ramberg–Osgood (RO) model as analytical tools. The findings derived from curve fitting exercises unequivocally underscore the superior applicability of the Ramberg–Osgood model, particularly in characterizing modulus reduction behavior. Conversely, the modified hyperbolic model emerges as the preferred choice for comprehensive damping ratio analyses. This study enhances the comprehension of rock dynamics and responses under diverse loading conditions, contributing valuable understanding to rock engineering. Insights into loading and strain rate effects aid informed decisions and preventive measures for rock deformation and collapse risks.</p>
38.	<p>Electron beam irradiation-induced atomically thin domes of two-dimensional materials: Graphene and MoS₂ M Pandey, R Ahuja, R Kumar - Surfaces and Interfaces, 2024</p> <p>Abstract: The local strain-induced indirect-to-direct band gap transition in bulk transition metal dichalcogenides (TMDCs) holds great potential for optoelectronic applications. The formation of domes on the topmost layer of a multilayered flake through hydrogen ion irradiation is an effective technique for tuning the band gap locally via molecular hydrogen (H₂) confinement. In this work, we present an alternative robust, simpler, and faster technique for concurrently forming and visualizing dome-like structures of two-dimensional (2D) materials through low-energy electron beam irradiation. We investigated the growth mechanism and dynamics of the domes under exposure to electron beams at different energy levels. The simultaneous production and imaging of atomically thin domes of 2D materials has several</p>

practical and fundamental applications, such as mass storage and transport, single photon emission, nano/micro-electromechanical sensors, strain engineering, etc.



[Emerging pollutant in surface water bodies: a review on monitoring, analysis, mitigation measures and removal technologies of micro-plastics](#)

A Gani, S Pathak, A Hussain... - Environmental Geochemistry and Health, 2024

39.

Abstract: Water bodies play a crucial role in supporting life, maintaining the environment, and preserving the ecology for the people of India. However, in recent decades, human activities have led to various alterations in aquatic environments, resulting in environmental degradation through pollution. The safety of utilizing surface water sources for drinking and other purposes has come under intense scrutiny due to rapid population growth and industrial expansion. Surface water pollution due to micro-plastics (MPs) (plastics < 5 mm in size) is one of the emerging pollutants in metropolitan cities of developing countries because of its utmost resilience and synthetic nature. Recent studies on the surface water bodies (river, pond, Lake etc.) portrait the correlation between the MPs level with different parameters of pollution such as specific conductivity, total phosphate, and biological oxygen demand. Fibers represent the predominant form of MPs discovered in surface water bodies, exhibiting fluctuations across seasons. Consequently, present study prioritizes understanding the adaptation, prevalence, attributes, fluctuations, and spatial dispersion of MPs in both sediment and surface water environments. Furthermore, the study aims to identify existing gaps in the current understanding and underscore opportunities for future investigation. From the present study, it has been reported that, the concentration of MPs in the range of 0.2–45.2 items/L at the Xisha Islands in the south China sea, whereas in India it was found in the range of 96 items/L in water samples and 259 items/kg in sediment samples. This would certainly assist the urban planners in achieving sustainable development goals to mitigate the increasing amount of emergent pollutant load.

[Enhanced electrocatalytic performance of bismuth-doped zinc stannate towards OER and HER through oxygen vacancies: p-block metal ion doping empowering d-block](#)

RT Parayil...K Garg, S Jangra...TC Nagaiah - Sustainable Energy and Fuels, 2024

40.

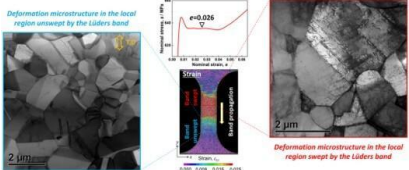
Abstract: In order to meet the future energy requirements of society, electrocatalytic water splitting is considered as one of the efficient methods to produce pure hydrogen fuel on a large scale. Doping has been established as a very effective strategy to engineer the active sites of electrocatalysts to improve their efficacy towards various electrochemical reactions. Herein, we have synthesized Zn_2SnO_4 doped with different metal ions such as Mn^{2+} , Bi^{3+} , Co^{3+} and Fe^{3+} and studied the electrocatalytic activities of these samples. Among the dopants investigated, Bi^{3+} exhibited the best catalytic activity towards hydrogen evolution reaction (HER) with good stability, high endurance and durability, with a faradaic efficiency (FE) of 88%. The $Zn_2SnO_4:Bi^{3+}$ composition also showed significant catalytic activity towards oxygen evolution reaction (OER) with a FE of 78%. Considering the bifunctional activity of the catalyst, a full cell was configured to carry out overall water splitting. The high catalytic activity of the bismuth-doped samples can be explained on the basis of enhanced electrochemically active surface area aided by the presence of high density of oxygen vacancies.

41.

[Enhancement of superconductivity in ZrS2C arising from phonon softening on transition from bulk to monolayer.](#)

P Jamwal, R Ahuja, R Kumar - Journal of Physics: Condensed Matter, 2024

	<p>Abstract: We report a new compound, Zr₂S₂C, belonging to the transition metal carbo-chalcogenide (TMCC) family. Through first-principles calculations, our analysis of phonon dispersion spectra indicates that the compound is dynamically stable in both bulk and monolayer forms. We systematically investigated the electronic structure, phonon dispersion, and electron-phonon coupling (EPC) driven superconducting properties in bulk and monolayer Zr₂S₂C. The results demonstrate the metallic character of bulk Zr₂S₂C, with a weak EPC strength (λ) of 0.41 and superconducting critical temperature (T_c) of ~ 3 K. The monolayer Zr₂S₂C has an enhanced λ of 0.62 and T_c of ~ 6.4 K. The increased λ value in the monolayer results from the softening of the acoustic phonon mode. We found that when biaxial strain is applied, the low energy acoustic phonon mode in monolayer becomes even softer. This softening leads to a transformation of the Zr₂S₂C monolayer from its initial weak coupling state ($\lambda = 0.62$) to a strongly coupled state, resulting in an increased λ value of 1.33. Consequently, the superconducting critical temperature experiences a twofold increase. These findings provide a theoretical framework for further exploration of the layered two-dimensional TMCC family, in addition to offering valuable insights.</p>
42.	<p>Existence and uniqueness of solution to unsteady Darcy-Brinkman problem with Korteweg stress for modelling miscible porous media flow S Kundu, SN Maharana, M Mishra - Journal of Mathematical Analysis and Applications, 2024</p> <p>Abstract: The work investigates a model that combines a convection-diffusion-reaction equation for solute concentration with an unsteady Darcy-Brinkman equation for the flow field, including the Korteweg stress. Additionally, the flow field experiences an external body force term while the permeability fluctuates with solute concentration. Such models are used to describe flows in porous mediums such as fractured karst reservoirs, mineral wool, industrial foam, coastal mud, etc. The system of equations has Neumann boundary conditions for the solute concentration and no-flow conditions for the velocity field, and the well-posedness of the model is discussed for a wide range of initial data. The proofing techniques remain applicable in establishing the well-posedness of non-reactive and homogeneous porous media flows under the specified simplifications.</p>
43.	<p>Experimental and numerical study of underwater laser transmission welding DK Goyal, R Kant - Optics and Laser Technology, 2024</p> <p>Abstract: This work demonstrates the feasibility of the underwater laser transmission welding (LTW) of polycarbonate sheets. The experiments are performed to investigate the effect of water depth, laser power, beam diameter, and scan speed on the weld strength, weld dimensions, and bond morphology. The results of mechanical properties and bond morphology of the weld joint in underwater are compared with air environment. The lap shear tests are performed to obtain the shear force–displacement of the welded joints. A three-dimensional (3-D) numerical model is developed to estimate the interface temperature in the underwater condition, which is validated by comparing the numerical weld width and weld depth with their corresponding experimental value. The bond morphology of the weldments is analyzed by the optical microscope and scanning electron microscopy (SEM). The results show that a maximum mean breaking force of 567.5 N is obtained at the 20 mm water depth which is 6 % higher than air due to lower thermal degradation and wider bubble-less region inside the welded region.</p>
44.	<p>Exploring potential of cold spray technology for medical devices: Current and future scenario A Kumar, S Rathor, M Vostrak, R Kant, H Singh... - Materials Today Communications, 2024</p> <p>Abstract: This review provides a comprehensive discussion on surface engineering of medical devices, with a central focus on the relatively new and innovative surface engineering technology, known as cold spray. The introduction sets the stage for the in-depth discussion on</p>

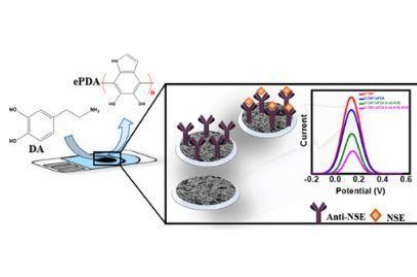
	<p>antimicrobial and biomedical surfaces, which highlights the importance of design and modification of medical device surfaces. Moreover, the current advancements in medical coatings and emerging trends are briefed that are shaping the future landscape of the medical coatings industry. The focus is on contemporary technologies, with a notable emphasis on the application of cold spray. The review also presents background information, bonding mechanisms, and process parameters involved in cold spray-based surface modification of various biomaterials. Moreover, a key question comprising whether cold spray can be a potential technology for medical device surface modifications has also been addressed. Additionally, the potential of cold spray for additive manufacturing of medical devices, such as the development of antimicrobial, biocompatible, and bioactive standalone products has been discussed. This review will serve as an important resource for researchers and practitioners interested in exploring the role of cold spray in advancing medical device manufacturing.</p>
<p>45.</p>	<p>Exploring unusual Lüders deformation in ultrafine-grained high-Mn austenitic steel S Hwang, H Kato, K Okada...Avala Lavakumar... - <i>Materials Research Letters</i>, 2024</p> <p>Abstract: Ultrafine-grained (UFG) high-Mn austenitic steel exhibited unusual discontinuous yielding on its stress-strain curve, characterized by a yield drop followed by a stress plateau, indicative of Lüders deformation. Utilizing the digital image correlation (DIC) technique, a strain-localized region known as a Lüders band was observed to propagate during Lüders deformation. Following microstructural observations using state-of-the-art techniques such as in-situ synchrotron XRD measurement during the tensile test and ex-situ S/TEM and SEM-ECCI, dislocation multiplication, rather than twinning, was theoretically identified as the primary deformation mechanism responsible for the unusual Lüders deformation in UFG high-Mn austenitic steel.</p>  <p>The figure consists of three parts: a stress-strain curve on the left showing a yield drop followed by a stress plateau; a central SEM-ECCI image showing a microstructure with a Lüders band; and a right SEM-ECCI image showing a similar microstructure. The stress-strain curve is labeled with $\sigma = 0.026$ and $\epsilon = 0.026$. The SEM-ECCI images are labeled with '2 μm' and 'Deformation microstructure in the local region swept by the Lüders band'.</p>
<p>46.</p>	<p>Green synthesis of organic nanomaterials and their applications A Sharma, A Kumar, R Singh... - <i>Biogenic Wastes-Enabled Nanomaterial Synthesis</i>, 2024</p> <p>Abstract: Nanotechnology is a rapidly evolving technology that is still in its infancy, but holds immense potential due to its various applications. It entails developing and use of materials that have dimensions inside the brackets of 1–100 nanometers. Nowadays, a wide range of physicochemical techniques are employed to synthesize organic nanoparticles (NPs). For many years, scientists have been experimenting with various synthetic approaches to create organic nanoparticles. When compared to chemical synthesis that utilizes dangerous diluents, elevated pressure, energy, and thermochemical methods, the green nanoparticle production technique is a more straightforward, efficient, and eco-friendly alternative. Sustainable process offers ecologically benign, easy, affordable, and systematic approach to nanoparticle synthesis. Given the vast range of uses for organic nanoparticles, as in environmental and medicinal domains, the utilization of green approaches is pivotal in the synthesis of NPs. The goal of sustainable synthesis is to reduce the utilization of toxic substances, for manufacturing nanoparticles. The basics of green chemistry are discussed here, as well as an overview of environmental-friendly synthesis of organic nanomaterials and their uses.</p>
<p>47.</p>	<p>Greening the future: identifying and mitigating environmental hotspots in the MSME sector - a wall mixer case study J Singh, S Gupta, S Jagtap - <i>International Journal of Sustainable Engineering</i>, 2024</p>

	<p>Abstract: In response to concerns about depleting natural resources, organisations are developing eco-friendly products and services. This study examines the role of manufacturing industries and services in sustainable resource utilisation, focusing on the Micro, Small, Medium Enterprises (MSME) sector, a significant contributor to global Gross Domestic Product (GDP). Using Life Cycle Assessment (LCA) methodology, the research identifies hotspots within the production processes of three companies manufacturing bathroom fittings, specifically the ‘Wall mixer’ component used in households and hotels. The study calculates CO2 equivalents for each phase of the product lifecycle, identifying average gate-to-gate process values across the companies. This comparison reveals specific hotspots, with a significant one identified, leading to recommendations for industries to prioritise this issue for immediate energy savings. The primary focus is to establish an initial benchmarking system to reduce CO2 equivalents in cradle-to-gate or gate-to-gate systems. Implementing these measures is expected to reduce the carbon footprint, energy consumption, and raw material usage, ultimately enhancing profitability for the three companies.</p>
48.	<p>High performance Pt-anchored MoS2 based chemiresistive ascorbic acid sensor A Biswas...G Bassi, M Kumar... - Nanotechnology, 2024</p> <p>Abstract: Ascorbic acid (AA), known as vitamin C, is a vital bioactive compound that plays a crucial role in several metabolic processes, including the synthesis of collagen and neurotransmitters, the removal of harmful free radicals, and the uptake of iron by cells in the human intestines. As a result, there is an absolute need for a highly selective, sensitive, and economically viable sensing platform for AA detection. Herein, we demonstrate a Pt-decorated MoS2 for efficient detection of an AA biosensor. MoS2 hollow rectangular structures were synthesized using an easy and inexpensive chemical vapor deposition approach to meet the increasing need for a reliable detection platform. The synthesized MoS2 hollow rectangular structures are characterized through field effect scanning electron microscopy (FESEM), energy-dispersive spectroscopy elemental mapping, Raman spectroscopy, and x-ray photoelectron spectroscopy. We fabricate a chemiresistive biosensor based on Pt-decorated MoS2 that measures AA with great precision and high sensitivity. The experiments were designed to evaluate the response of the Pt-decorated MoS2 biosensor in the presence and absence of AA, and selectivity was evaluated for a variety of biomolecules, and it was observed to be very selective towards AA. The Pt-MoS2 device had a higher response of 125% against 1 mM concentration of AA biomolecules, when compared to that of all other devices and 2.2 times higher than that of the pristine MoS2 device. The outcomes of this study demonstrate the efficacy of Pt-decorated MoS2 as a promising material for AA detection. This research contributes to the ongoing efforts to enhance our capabilities in monitoring and detecting AA, fostering advancements in environmental, biomedical, and industrial applications</p>
49.	<p>High strain rate testing of hybrid TPMS structures AI Ansari, NA Sheikh, N Kumar - Journal of the Brazilian Society of Mechanical Sciences and Engineering, 2024</p>

	<p>Abstract: This study provides an overview of the most recent advancements in the production of triple periodic minimal (TPMS) structure combinations of periodic surfaces and strut structures using an acrylonitrile butadiene styrene material and studies of their structural mechanics and energy absorption properties at high strain rates using split Hopkinson pressure bars. The simulation and experimental structural study of the Schwartz diamond (periodic surface) and Hybrid Schwartz diamond (HSD-periodic surface+strut) TPMS foam structures under quasistatic and dynamic loading conditions, as well as the behavior of the structures in terms of energy absorption and plateau stress from low to high strain rates, were performed. This study provides techniques for predicting the mechanical properties of combinations of periodic surface and strut structure-based TPMS structures made by FDM, as well as a better understanding of the possibilities and limitations of these structures. At low to high strain rates, each of the two structural crashworthiness features of the TPMS design were successfully recognized, analyzed, and documented.</p>
50.	<p>Identification and diagnosis of cervical cancer using a hybrid feature selection approach with the bayesian optimization-based optimized catboost classification algorithm J Dhar, S Roy - Journal of Ambient Intelligence and Humanized Computing, 2024</p> <p>Abstract: Cervical cancer is the most prevailing woman illness globally. Since cervical cancer is a very preventable illness, early diagnosis exhibits the most adaptive plan to lessen its global responsibility. However, because of infrequent knowledge, shortage of access to pharmaceutical centers, and costly schemes worldwide, most probably in emerging nations, the vulnerable subject populations cannot regularly experience the test. So, we need a clinical screening analysis to diagnose cervical cancer early and support the doctor to heal and evade cervical cancer's spread in women's other organs and save several lives. Thus, this paper introduces a novel hybrid approach to solve such problems: a hybrid feature selection approach with the Bayesian optimization-based optimized CatBoost (HFS-OCB) method to diagnose and predict cervical cancer risk. Genetic algorithm and mutual information approaches utilize feature selection methodology in this suggested research and form a hybrid feature selection (HFS) method to generate the most significant features from the input dataset. This paper also utilizes a novel Bayesian optimization-based hyperparameter optimization approach: optimized CatBoost (OCB) method to provide the most optimal hyperparameters for the CatBoost algorithm. The CatBoost algorithm is used to classify cervical cancer risk. There are two real-world, publicly available cervical cancer-based datasets utilized in this suggested research to evaluate and verify the suggested approach's performance. A 20-fold cross-validation strategy and a renowned performance evaluation metric are utilized to assess the suggested approach's performance. The outcome implies that the possibility of forming cervical cancer can be efficiently foretold using the suggested HFS-OCB method. Therefore, the suggested approach's indicated result is compared with the other algorithms and provides the prediction. Such a predicted result shows that the suggested approach is more capable, reliable, scalable, and more effective than the other machine learning algorithms.</p>
51.	<p>Internet of things enabled adjustable ramp system for productivity enhancement of micro, small and medium enterprises A Sharma, B Singh, P Sarkar - Engineering Proceedings, 2024</p> <p>Abstract: The industry usually faces a problem during the loading/unloading of finished products and raw materials from one place to another when both places are at different elevations. As trucks are of variable height and industry loading bays are at different elevations, it is not possible to drive the pallets effectively into freight, which results in decreasing loading/unloading efficiency of small concerns. In this paper, an adjustable height ramp system for increasing production efficiency and improving the industrial working environment was developed using a linear actuator and automation system for the safe loading and unloading of</p>

	<p>pallets. This adjustable ramp will help to increase the productivity of micro, small and medium enterprises (MSMEs), and it will provide a safe working environment. Using an adjustable ramp will help create a bridge between industry loading bays and freight, and it will also resolve the issue of different heights of both by making a path between them. The Internet of things (IoT)-enabled lifting and downward movement of the ramp is attempted for oil/air filter MSMEs.</p>
52.	<p>Investigation of the adsorption behaviour of toxic heavy metals and bacteria on two allotropes of low dimensional boron nitride: Implications for detection and elimination B Roondhe, R Ahuja, W Luo - Applied Surface Science, 2024</p> <p>Abstract: In this research, the focus was on two 2D allotropes of boron nitride (BN), specifically Haeck-BN and Twin-BN. They exhibit unique structural and electronic characteristics, making them suitable for sensing applications. High surface area materials offer numerous affinity sites for heavy metal ions and toxic molecules. Using density functional theory (DFT), the adsorption mechanisms of various contaminants in gas (solvent) phase on both pristine and doped Haeck-BN and Twin-BN were investigated. Pronounced adsorption of arsenic (As) and lead (Pb) was observed on pristine Twin-BN sheets, with adsorption energies of -2.83 eV (-2.86 eV) and -2.03 eV (-2.39 eV), respectively. Haeck-BN showed weaker interactions, with adsorption energies of -1.48 eV (-1.55 eV) for As and -0.64 eV (-0.92 eV) for Pb. Significant adsorption of specific amino acids, integral components of bacterial cell walls, was noted on both pristine and silver-modified sheets. The electronic properties showed significant shifts upon molecular adsorption, confirming their sensitivity towards foreign contaminants. The high adsorption energies of amino acids suggest potential applications in efficient bacterial inactivation for water purification. While real-world scenarios pose challenges, the calculations provide valuable insights for potential use of these nanosheets in advanced water purification membrane technology.</p>
53.	<p>Isolated single photon emitters with low Huang-Rhys factor in hexagonal boron nitride at room temperature A Bhunia...N Singh, B Chakraborty, RV Nair - Journal of Physics D: Applied Physics, 2024</p> <p>Abstract: Development of stable room-temperature bright single-photon emitters using atomic defects in hexagonal-boron nitride flakes (h-BN) provides significant promises for quantum technologies. However, an outstanding challenge in h-BN is creation and detection of isolated, stable single photon emitter with high emission rate and with very low Huang-Rhys (HR) factor. Here, we discuss the quantum photonic properties of single, isolated, stable quantum emitter that emit single photons with a high emission rate and low HR value of 0.6 ± 0.2 at room temperature. Scanning confocal image confirms the presence of a deserted, single quantum emitter with prominent zero-phonon line at ~ 578 nm with well-separated phonon sideband at 626 nm. The second-order intensity-intensity correlation measurement shows an anti-bunching dip of ~ 0.25 with an emission lifetime of 2.46 ± 0.1 ns, reinforcing distinct features of single photon emitter. The importance of low-energy electron beam irradiation and subsequent annealing is emphasized to achieve stable, reproducible single photon emitters.</p>
54.	<p>Label-free assessment of neuron-specific enolase via polydopamine over a carbon-nanotube-based flexible immunosensor D Mehta, N Thakur, TC Nagaiah - ACS Applied Bio Materials, 2024</p> <p>Abstract: A label-free electrochemical immunosensor was developed for the rapid and sensitive detection of neuron-specific enolase (NSE). The electropolymerization of dopamine in conjunction with highly conductive carbon nanotubes offers a simple and quick platform for the direct anchoring of antibodies without the assistance of any coupling agent as well as a blocking agent. The developed immunosensor exhibited a wider detection range from 120 pM (9 ng mL$^{-1}$) to 3 nM (200 ng mL$^{-1}$) for NSE with a high sensitivity of 3.9 μA pM$^{-1}$ cm$^{-2}$ in 0.1 M</p>

phosphate-buffered saline (PBS) at physiological pH (7.4). Moreover, the short recognition time (15 min) for the antigen enabled the detection to be fast and less invasive. Additionally, the evaluation of a rate constant at various concentrations of NSE via feedback mode of scanning electrochemical microscopy (SECM) explained the profound effect of antigen concentration on the rate of flow of electrons. Therefore, the proposed immunosensor can be a promising tool for the early detection of small cell lung cancer in a very short period of time with consistent accuracy.



[Large out-of-plane spin-orbit torque in topological Weyl semimetal TaIrTe4](#)
 L Bainsla, B Zhaao, N Behera, A M. Hoque,... - Nature Communications, 2024

55.

Abstract: The unique electronic properties of topological quantum materials, such as protected surface states and exotic quasiparticles, can provide an out-of-plane spin-polarized current needed for external field-free magnetization switching of magnets with perpendicular magnetic anisotropy. Conventional spin-orbit torque (SOT) materials provide only an in-plane spin-polarized current, and recently explored materials with lower crystal symmetries provide very low out-of-plane spin-polarized current components, which are not suitable for energy-efficient SOT applications. Here, we demonstrate a large out-of-plane damping-like SOT at room temperature using the topological Weyl semimetal candidate TaIrTe4 with a lower crystal symmetry. We performed spin-torque ferromagnetic resonance (STFMR) and second harmonic Hall measurements on devices based on TaIrTe4/Ni80Fe20 heterostructures and observed a large out-of-plane damping-like SOT efficiency. The out-of-plane spin Hall conductivity is estimated to be $(4.05 \pm 0.23) \times 10^4 (\hbar/2e) (\Omega\text{m})^{-1}$, which is an order of magnitude higher than the reported values in other materials.

[Measurements of fission fragments in the interaction of 19F + 181Ta system at 115 MeV](#)
 S Arora, MK Sharma, SK Gautam...PP Singh... - Journal of Radioanalytical and Nuclear Chemistry, 2024

56.

Abstract: This paper details the cross-section measurements of 38 fission-like events in 19F + 181Ta system at energy 115 MeV, originating from complete and/or incomplete fusion-fission processes. The recoil-catcher off-beam activation technique followed by γ -ray spectroscopy has been used to measure production cross sections of fission-like events. The measured cross-section data of fission-like events align well with Gaussian distributions indicating their production via de-excitation of equilibrated compound nucleus formed. Additionally, the study explores mass and isotopic yield distributions of fission fragments, with the presently measured isotopic yield variance which is found to be consistent with literature values for other fissioning systems.

[Multiscale effects of the calcimimetic drug, etelcalcetide on bone health of rats with secondary hyperparathyroidism induced by chronic kidney disease](#)
 S Sharma, S Kumar, M S Tomar...N Kumar... - Bone, 2024

57.

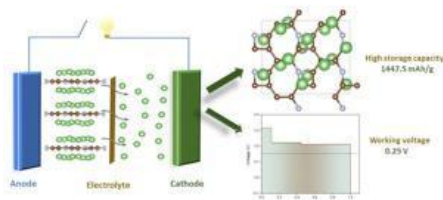
Abstract: Chronic kidney disease-induced secondary hyperparathyroidism (CKD-SHPT) heightens fracture risk through impaired mineral homeostasis and elevated levels of uremic toxins (UTs), which in turn enhance bone remodeling. Etelcalcetide (Etel), a calcium-sensing receptor (CaSR) agonist, suppresses parathyroid hormone (PTH) in hyperparathyroidism to

reduce excessive bone resorption, leading to increased bone mass. However, Etel's effect on bone quality, chemical composition, and strength is not well understood. To address these gaps, we established a CKD-SHPT rat model and administered Etel at a human-equivalent dose concurrently with disease induction. The effects on bone and mineral homeostasis were compared with a CKD-SHPT (vehicle-treated group) and a control group (rats without SHPT). Compared with vehicle-treated CKD-SHPT rats, Etel treatment improved renal function, reduced circulating UT levels, improved mineral homeostasis parameters, decreased PTH levels, and prevented mineralization defects. The upregulation of mineralization-promoting genes by Etel in CKD-SHPT rats might explain its ability to prevent mineralization defects. Etel preserved both trabecular and cortical bones with attendant suppression of osteoclast function, besides increasing mineralization. Etel maintained the number of viable osteocytes to the control level, which could also contribute to its beneficial effects on bone. CKD-SHPT rats displayed increased carbonate substitution of matrix and mineral, decreased crystallinity, mineral-to-matrix ratio, and collagen maturity, and these changes were mitigated by Etel. Further, Etel treatment prevented CKD-SHPT-induced deterioration in bone strength and mechanical behavior. Based on these findings, we conclude that in CKD-SHPT rats, Etel has multiscale beneficial effects on bone that involve remodeling suppression, mineralization gene upregulation, and preservation of osteocytes.

[N-doped biphenylene monolayer as high-performance 2D electrode material for Li-ion batteries](#)
M Kaur, Nidhi Duhan, TJ Dhilip Kumar - Journal of Energy Storage, 2024

58.

Abstract: Incorporating heteroatoms into the two-dimensional lattices of materials like biphenylene leads to groundbreaking advancements in material science, imparting extraordinary properties to the base material. In this study, a two-dimensional carbon lattice doped with nitrogen atoms, known as N-doped biphenylene (N-BPN), has been explored. Its potential utilization as an anode in secondary lithium-ion batteries (LIBs) has been showcased. Density Functional Theory (DFT) computations reveal that the N-doped biphenylene monolayer possesses a stable composition that remains resilient under dynamic, thermal, and mechanical conditions, exhibiting consistent metallic properties. The density of states study validates the monolayer's metallic properties, further enhancing its suitability for utilization as an electrode. The mean adsorption energies for consecutive adsorption of the lithium atom (adatom) onto the monolayer were found to vary between -0.91 to -0.20 eV, leading to a transfer of 0.87 from lithium to the monolayer. N-doped monolayer offers a minimal migration barrier of 0.20 eV and an elevated diffusion coefficient of 4.18×10^{-5} cm²s⁻¹. The migration of Li-ion onto the monolayer suggests an active charge/discharge process. N-BPN monolayer attained a high storage capacity of the order 1447.5 mAhg⁻¹, a low working voltage of 0.25 V, and extremely high energy densities of 4038.52 mWhg⁻¹. In light of the collective findings of this study, it is evident that the N-BPN monolayer shows significant promise for serving as electrode material in LIBs for further generations.



[Novel hard and unusual superconducting monoclinic phase of FeB₂C₂: An ab initio evolutionary study](#)

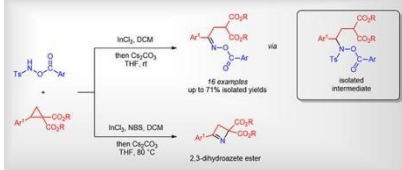
K Kotmool, U Pinsook, W Luo, R Ahuja... - Journal of Applied, 2024

59.

Abstract: This study focuses on conducting an ab initio evolutionary investigation to search for stable polymorphs of iron diborocarbides with the formula . We also examined other forms of C contents, including C and . Our findings reveal that the lowest energetic structure of is a

	<p>semimetallic monoclinic phase with a space group (s.g.) of C2/m and a metastable metallic phase of is an orthorhombic structure with s.g. of Pmmm. In addition, structural and relative properties of C and are performed and discussed to compare with . All predicted structures are dynamically and elastically stable, verified without negative phonon frequency and Born criteria, respectively. We also analyzed the energetic stability through calculated cohesive and formation energies, which showed that C2/m- is stable at low pressure. Interestingly, the C2/m and Pmmm phases of are hard materials with Vickers hardness () of 22.40 and 27.52 GPa, respectively. Additionally, we examined the electron–phonon coupling of both phases. Unexpectedly, we found that the semimetallic C2/m- phase is a superconductor with a significant superconducting temperature () exceeding 6 K. These findings provide some novel results for the Fe–B–C system and pave the way for investigating other metal borocarbides and related ternary compounds.</p>
60.	<p>On interpretation of fourier coefficients of Zagier type lifts V Kalia - Archiv der Mathematik, 2024</p> <p>Abstract: Jeon, Kang, and Kim defined the Zagier lifts between harmonic weak Maass forms of negative integral weights and half integral weights. These lifts were defined by establishing that traces related to cycle integrals of harmonic weak Maass forms of integral weights appear as Fourier coefficients of harmonic weak Maass forms of half integral weights. For fundamental discriminants d and they studied $-d$-th Fourier coefficients of the d-th Zagier lift with respect to the condition that is not a perfect square. For being a perfect square, the interpretation of coefficients in terms of traces is not possible due to the divergence of cycle integrals. In this paper, we provide an alternate definition of traces called modified trace in the condition that is a perfect square and interpret such coefficients in terms of the modified trace.</p>
61.	<p>Optical non-linearities and applications of ZnS phosphors A Chauhan, R Sharma, M Singh, R Sharma - Advanced Optical Technologies, 2024</p> <p>Abstract: Optical non-linearities play a crucial role in enabling efficient and ultrafast switching applications that are essential for next-generation photonic devices. ZnS phosphor material produces the best results in terms of increased luminescence quantum yield when doped with certain impurities. Nevertheless, the investigation of the third-order non-linear optical susceptibility of the phosphor materials can be exploited for various switching applications. In this regard, we review the recent advancements in the investigation of non-linear optical properties of ZnS phosphors, where the knowledge of absorption and refraction is utilized in various optical and detector applications. Furthermore, the review highlights strategies employed to enhance the non-linear optical response of phosphor materials as well as a general discussion of an attosecond optical switching scheme which can be used to fabricate devices with petahertz speeds. Consequently, we provide a solution to the unsolved problem of the significant extension of optical limiting applications to switching applications by developing design strategies to manipulate conventional ZnS phosphor material. The potential challenges and future prospects of utilizing phosphor materials for switching applications are also addressed. The strategies for manipulating ZnS phosphor can be generalized for a broad range of other materials by minimizing linear and non-linear losses, while enhancing the values of the non-linear refractive index coefficient. We propose that the figure-of-merit of ZnS material can be enhanced by using a suitable combination of pump and probe wavelength values, which can be useful for optical switching applications.</p>
62.	<p>Optimal sampling of spatial patterns improves deep learning-based early warning signals of critical transitions S Deb, E Mahendru, P Goyal, V Guttal...PS Dutta... - Royal Society Open Science, 2024</p> <p>Abstract: Complex spatio-temporal systems like lakes, forests and climate systems exhibit alternative stable states. In such systems, as the threshold value of the driver is crossed, the</p>

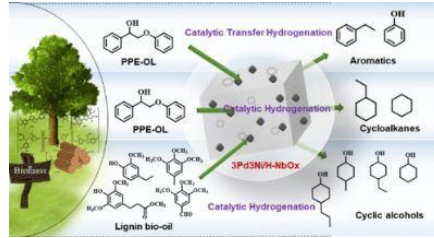
	<p>system may experience a sudden (discontinuous) transition or smooth (continuous) transition to an undesired steady state. Theories predict that changes in the structure of the underlying spatial patterns precede such transitions. While there has been a large body of research on identifying early warning signals of critical transitions, the problem of forecasting the type of transitions (sudden versus smooth) remains an open challenge. We address this gap by developing an advanced machine learning (ML) toolkit that serves as an early warning indicator of spatio-temporal critical transitions, Spatial Early Warning Signal Network (S-EWSNet). ML models typically resemble a black box and do not allow envisioning what the model learns in discerning the labels. Here, instead of naively relying upon the deep learning model, we let the deep neural network learn the latent features characteristic of transitions via an optimal sampling strategy (OSS) of spatial patterns. The S-EWSNet is trained on data from a stochastic cellular automata model deploying the OSS, providing an early warning indicator of transitions while detecting its type in simulated and empirical samples.</p>
63.	<p>Photoredox Catalysis by 21-Thiaporphyrins: A green and Efficient Approach for C-N Borylation and C-H Arylation I Gupta, A Janaagal, A Kushwaha, P Jhaldiyal, TJ Dhillip Kumar - Chemistry, 2024</p> <p>Abstract: The photocatalytic C-N borylation and C-H arylation mostly depend on the ruthenium and iridium complexes or eosin Y and the use of porphyrin catalysts is still in infancy. A series of novel 21-thiaporphyrins (A2B2 and A3B type) were synthesized having carbazole/phenothiazine moieties at their meso-positions and screened as catalysts for C-N borylation and C-H arylation. This paper demonstrates the 21-thiaporphyrin catalyzed C-N borylation and het-arylation of anilines under visible light. The method utilizes only 0.1 mol% of 21-thiaporphyrin catalyst under blue light for the direct C-N borylation and het-arylation reactions. A variety of substituted anilines were used as source for expensive and unstable aryl diazonium salts in the reactions. The heterobiaryls and aryl boronic esters were obtained in decent yields (up to 88%). Versatility of the 21-thiaporphyrin catalyst was tested by thiolation and selenylation of anilines under similar conditions. Mechanistic insight was obtained from DFT studies, suggesting that 21-thiaporphyrin undergo an oxidative quenching pathway. The photoredox process catalyzed by 21-thiaporphyrins offers a mild, efficient and metal-free alternative for the formation of C-C, C-S, and C-Se bonds in aryl compounds; it can also be extended to borylation reaction.</p>
64.	<p>Predictive design of novel nickel-based superalloys beyond Haynes 282 G Ouyang, O Palasyuk, P Singh, PK Ray,... - Acta Materialia, 2024</p> <p>Abstract: Nickel-based superalloys are in great demand for harsh-service conditions involving high temperatures and oxidative environments. Haynes 282 stands out due to its excellent high-temperature properties and easy fabricability. However, the upper operation temperature of Haynes 282 is limited due to its relatively low liquidus temperature. Equipped with high-fidelity density-functional theory calculations and high-throughput experimentation methodology, we explored new compositional spaces that exhibit higher liquidus temperature and higher strength. While maintaining the manufacturability, the newly designed alloy shows improved strength and ductility at room temperature and better oxidation resistance up to 800 °C. The new compositions showcase a minor change in the refractory and metalloid content can significantly impact the mechanical and oxidation performance of superalloys.</p>
65.	<p>Recent advances in the therapeutic applications of selenium nanoparticles JA Ansari, JA Malik, S Ahmed, M Manzoor,... - Molecular Biology Reports, 2024</p> <p>Abstract: Selenium nanoparticles (SeNPs) are an appealing carrier for the targeted delivery. The selenium nanoparticles are gaining global attention because of the potential therapeutic applications in several diseases e.g., rheumatoid arthritis (RA), inflammatory bowel disease (IBD), asthma, liver, and various autoimmune disorders like psoriasis, cancer, diabetes, and a</p>

	<p>variety of infectious diseases. Despite the fact still there is no recent literature that summarises the therapeutic applications of SeNPs. There are some challenges that need to be addressed like finding targets for SeNPs in various diseases, and the various functionalization techniques utilized to increase SeNP's stability while facilitating wide drug-loaded SeNP distribution to tumor areas and preventing off-target impacts need to focus on understanding more about the therapeutic aspects for better understanding the science behind it. Keeping that in mind we have focused on this gap and try to summarize all recent key targeted therapies for SeNPs in cancer treatment and the numerous functionalization strategies. We have also focused on recent advancements in SeNP functionalization methodologies and mechanisms for biomedical applications, particularly in anticancer, anti-inflammatory, and anti-infection therapeutics. Based on our observation we found that SeNPs could potentially be useful in suppressing viral epidemics, like the ongoing COVID-19 pandemic, in complement to their antibacterial and antiparasitic uses. SeNPs are significant nanoplatfroms with numerous desirable properties for clinical translation.</p>
66.	<p>Reliability of early warning indicators of critical transition in stochastic Van der Pol oscillators with additive correlated noise N Vishnoi, V Gupta, A Saurabh, L Kabiraj - Nonlinear Dynamics, 2024</p> <p>Abstract: We conduct a numerical investigation to assess the effect of noise characteristics on early warning indicators (EWIs) of critical transition in Van der Pol oscillators undergoing supercritical and subcritical Hopf bifurcation. Our study primarily focuses on the effects of additive correlated noise modeled by the OU process in the stable (subthreshold) region and corresponding trends in EWIs based on signal amplitude distribution, frequency spectra, fractal, and complexity measures as the system is brought closer to bifurcation, as a function of noise color and intensity. Our results indicate that the coherence factor is a reliable indicator for the entire range of investigated noise color, while variance and decay rates of the autocorrelation function are reliable when noise correlation times are either much smaller or larger than the system time scale. Kurtosis, permutation entropy and Jensen-Shannon complexity can be effectively employed in systems where noise exhibits minimal correlation time (resembling white noise). While the Hurst exponent proves a reliable indicator in systems where noise has correlation times much larger than the time scale of the system, multi-fractal spectrum width and skewness are deemed unsuitable as EWIs. These insights enhance our understanding of the effectiveness and limitations of various EWIs in forecasting critical transitions within dynamical systems.</p>
67.	<p>Ring-opening of donor-acceptor cyclopropane diester for the synthesis of oxime esters and 2,3-dihydroazete ester N Yadav, K Verma, A Das, N Kaur, P Banerjee - Synthesis, 2024</p> <p>Abstract: A simple and efficient approach for the synthesis of privileged oxime esters by employing donor-acceptor cyclopropane diesters (DACs) as one of the potential precursors is reported. The strategy involves Lewis acid catalyzed ring-opening of DACs, resulting in an open-chain intermediate followed by the base-mediated construction of the corresponding oxime esters in a one-pot reaction. Moreover, the process also features the synthesis of diethyl 4-(4-methoxyphenyl)azete-2,2(3H)-dicarboxylate.</p> 
68.	<p>Seismic response assessment of ductile reinforced concrete columns affected by corrosion and axial load variationsx</p>

	<p>SN Amini, AS Rajput - Structures, 2024</p> <p>Abstract: The present study investigates the effect of reinforcement corrosion and axial compression ratio (ACR) on the seismic response of large-scale ductile reinforced concrete (RC) columns. 3D numerical models of sound and corroded RC columns were developed and validated with detailed experimentation. Various parameters, such as hysteresis and backbone curves, stiffness degradation, ductility, and energy dissipation, were evaluated for all the specimens. The numerical findings were then compared with the experimental findings. Subsequently, a thorough parametric study was executed to analyse the structural behaviour under varying corrosion degrees and ACR level combinations. It was observed that both sound and corroded specimens experienced significant degradation in terms of their strength, deformability, stiffness, and ductility due to elevated ACR levels. Moreover, increased ACR levels in both specimen types led to a decline in pre-peak and post-peak response trajectories, resulting in an early achievement of peak response at lower drift levels. The study's outcome advocates the significance of incorporating ACR levels into the design philosophy of ductile reinforcements for RC columns.</p>
69.	<p><u>Silver and copper nanoparticle-loaded self-assembled pseudo-peptide thiourea-based organic-inorganic hybrid gel with antibacterial and superhydrophobic properties for antifouling surfaces</u></p> <p>R Devi, G Singh, A Singh, J Singh,...N Singh - ACS Applied Bio Materials, 2024</p> <p>Abstract: The escalating threat of antimicrobial resistance has become a global health crisis. Therefore, there is a rising momentum in developing biomaterials with self-sanitizing capabilities and inherent antibacterial properties. Despite their promising antimicrobial properties, metal nanoparticles (MNPs) have several disadvantages, including increased toxicity as the particle size decreases, leading to oxidative stress and DNA damage that need consideration. One solution is surface functionalization with biocompatible organic ligands, which can improve nanoparticle dispersibility, reduce aggregation, and enable targeted delivery to microbial cells. The existing research predominantly concentrates on the advancement of peptide-based hydrogels for coating materials to prevent bacterial infection, with limited exploration of developing surface coatings using organogels. Herein, we have synthesized organogel-based coatings doped with MNPs that can offer superior hydrophobicity, oleophobicity, and high stability that are not easily achievable with hydrogels. The self-assembled gels displayed distinct morphologies, as revealed by scanning electron microscopy and atomic force microscopy. The cross-linked matrix helps in the controlled and sustained release of MNPs at the site of bacterial infection. The synthesized self-assembled gel@MNPs exhibited excellent antibacterial properties against harmful bacteria such as Escherichia coli and Staphylococcus aureus and reduced bacterial viability up to 95% within 4 h. Cytotoxicity testing against metazoan cells demonstrated that the gels doped with MNPs were nontoxic ($IC_{50} > 100 \mu M$) to mammalian cells. Furthermore, in this study, we coated the organogel@MNPs on cotton fabric and tested it against Gram +ve and Gram -ve bacteria. Additionally, the developed cotton fabric exhibited superhydrophobic properties and developed a barrier that limits the interaction between bacteria and the surface, making it difficult for bacteria to adhere and colonize, which holds potential as a valuable resource for self-cleaning coatings.</p>
70.	<p><u>The shape of the $T_z=+1$ nucleus ^{94}Pd and the role of proton-neutron interactions on the structure of its excited states</u></p> <p>A Yaneva, S Jazrawi, M. Mikołajczuk... A Sharma... - Physics Letters B, 2024</p> <p>Abstract: Reduced transition probabilities have been extracted between excited, yrast states in the $N=Z+2$ nucleus ^{94}Pd. The transitions of interest were observed following decays of the $\pi\pi=14+$, $E_x=2129$-keV isomeric state, which was populated following the projectile</p>

	<p>fragmentation of a ^{124}Xe primary beam at the GSI Helmholtzzentrum für Schwerionenforschung accelerator facility as part of FAIR Phase-0. Experimental information regarding the reduced E2 transition strengths for the decays of the yrast 8^+ and 6^+ states was determined following isomer-delayed $E\gamma_1-E\gamma_2-\Delta T_{2,1}$ coincidence method, using the $\text{LaBr}_3(\text{Ce})$-based FATIMA fast-timing coincidence gamma-ray array, which allowed direct determination of lifetimes of states in ^{94}Pd using the Generalized Centroid Difference (GCD) method. The experimental value for the half-life of the yrast 8^+ state of 755(106) ps results in a reduced transition probability of $B(E2:8^+ \rightarrow 6^+) = 205-25+34 e^2 \text{ fm}^4$, which enables a precise verification of shell-model calculations for this unique system, lying directly between the $N=Z$ line and the $N=50$ neutron shell closure. The determined ($E2$) value provides an insight into the purity of ($g9/2$) configurations in competition with admixtures from excitations between the (lower) $N=3pf$ and (higher) $N=4gds$ orbitals for the first time. The results indicate weak collectivity expected for near-zero quadrupole deformation and an increasing importance of the $T=0$ proton-neutron interaction at $N=48$.</p>
71.	<p>The spatial footprint of financial assistance to poor households in India: a district-level analysis S Agarwal, SR Behera - Finance and Space, 2024</p> <p>Abstract: The key focus of the United Nations' Sustainable Development Goals (SDG 1), target 1.3, is to implement appropriate social protection systems with substantial coverage of the poor and vulnerable people by 2030. According to the United Nations Development Programme's (UNDP) The Global Multidimensional Poverty Index (2022) survey data, 16.4% of the population in India is multidimensionally poor, while an additional 18.7% of the population is classified as most vulnerable to multidimensional poverty. This paper visualises the geospatial distribution of beneficiaries below the poverty line receiving basic income support from the Indian government across districts in the financial year 2022–23. The results exhibit that beneficiaries are geographically concentrated in specific districts, and the positive effects of basic income support benefit adjacent regions in rural India. In urban India, beneficiaries are confined to some districts, and the benefits of basic income support do not extend to adjacent districts. Policy should focus on identifying districts that lag in receiving basic income support and give them priority to enhance the distribution system of national social assistance programmes in India.</p>
72.	<p>The synergy of alloyed Pd and Ni Over H-NbOx: Enhancing hydrogenation of lignin derivatives and lignin bio-oil into cyclic hydrocarbons and alcohols GS More, R Bal, R Srivastava - ACS Sustainable Chemistry & Engineering, 2024</p> <p>Abstract: The study aims to investigate the hydrogenation of lignin-derived bio-oil (known as lignin bio-oil) and β-O-4 linkages, which are representative lignin model compounds. The hydrogenation of these molecules produces cyclic hydrocarbons and aromatic platform chemicals. H-NbOx was synthesized using a hydrothermal method, followed by an acid treatment of Nb_2O_5. Three wt % Pd and 3 wt % Ni were deposited over H-NbOx to form an alloyed PdNi/H-NbOx catalyst. XPS, NH_3-TPD, and O_2-TPD revealed intrinsic active sites, metal-support interactions, and modified oxygen vacancies, making it highly efficient for the hydrogenation of 2-phenoxy-1-phenylethanol (PPE-OL) in dodecane using 3 MPa hydrogen. The hydrogenation of PPE-OL yielded >98% cyclic hydrocarbons (cyclohexane and ethyl cyclohexane). In contrast, 3Pd/H-NbOx and 3Ni/H-NbOx showed varied selectivity, producing a mixture of ethylbenzene, phenol, ethyl cyclohexane, and cyclohexanol. Notably, catalytic transfer hydrogenation (CTH) resulted in the formation of >99% aromatics (phenol and ethylbenzene) in isopropanol. Expanding the investigation from model compounds, PdNi/H-NbOx was utilized to hydrogenate lignin bio-oil derived from wheat straw, yielding saturated cyclic alcohols with a high yield at 250 °C in isopropanol. It underscores the potential of the developed protocol to</p>

effectively meet energy demands by generating aromatics via catalytic transfer hydrogenation and cyclic hydrocarbons via hydrogenation.



[Transition and postfault correction strategy for a single-phase inverter with improved redundant leg utilization](#)

PS Bhakar, J Kalaiselvi, NBY Gorla... - IEEE Transactions on Industrial Electronics, 2024

73.

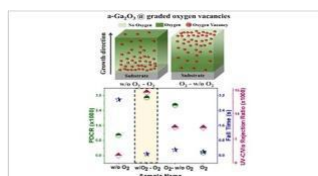
Abstract: Single-phase inverters are frequently employed in several applications with redundant switches, legs, or modules in the circuit. In this article, a transition scheme is developed which uses a redundant leg to achieve two distinct goals namely ripple compensation and fault tolerance in the inverter unit. To account for the second-harmonic ripple (SHR) using a redundant leg, a pre-fault control technique is created which ensures 0% to 100% compensation of the SHR in the dc-link current, minimizing the stress on the dc-link capacitor. On occurrence of a fault, the transition scheme securely switches the inverter operation from the pre-fault condition (ripple compensation mode) to the post-fault correction (fault-tolerant mode) in the preparation stage using the same redundant leg. The inclusion of connecting devices and the modifications on the ac side filter are competent with the pre-fault and the post-fault condition. The proposed transition and the correction scheme are tested on a single-phase inverter for different fault conditions.

[Vertically graded oxygen vacancies in amorphous Ga2O3 for offsetting the conventional trade-off between photoresponse and response time in solar-blind photodetectors](#)

D Kaur, R Dahiya, N Ahmed, M Kumar - ACS Applied Electronic Materials, 2024

74.

Abstract: Recently, amorphous Ga₂O₃-based photodetectors are garnering interest for their relative ease-of-growth at room temperature and their virtuous use in flexible electronics. However, a major concern that remains is the huge trade-off between key performance parameters, viz., photoresponse and response time. Being replete with oxygen vacancies, acting as trap centers, devices usually boast a large photoresponse but at the cost of longer response time due to prolonged carrier recombination. Most of remedial measures to offset this trade-off include oxygen vacancy engineering but in a continuous manner, implying creating/deleting vacancies throughout the film thickness, leading to a change in only one of the parameters. Herein, we propose defect engineering in amorphous Ga₂O₃ by grading oxygen vacancies using an intermittent oxygen supply. XPS depth profile studies confirm gradation of vacancies, which may be accessed by applying a different bias, in resonance with electric field distribution simulations. Graded vacancy films show negligible persistent photoconductivity, a high PDCR of 3×10^3 , a high UV–vis rejection ratio of 1.49×10^4 , and a fast fall time of 85 ms as opposed to continuous supply films, which show either high photoresponse or fast speed (in seconds). This work provides a way to use graded oxygen vacancies as tool in defect engineering to offset the trade-off and achieve high photoresponse and fast response time in amorphous Ga₂O₃ films simultaneously.

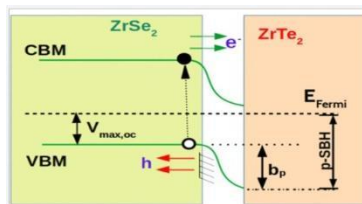


75.

[Zirconium dichalcogenide-based van der waals heterostructures for efficient schottky barrier solar cells](#)

L Tatikondewar, S Chakraborty, R Ahuja, A Kshirsagar - ACS Applied Energy Materials, 2024

Abstract: We present our study of bilayered heterostructures consisting of a metallic ZrTe₂(1T) monolayer and a semiconducting ZrSe₂(1T) monolayer leading to a bilayered Schottky contact. We have confirmed the dynamic stability of this bilayered heterostructure using phonon dispersion spectra and the structural stability from the binding energy value. We have performed ladder calculations, namely, density functional theory for structural relaxation and electronic self-consistency; final electronic structure for better estimation of the band gap with single-shot GW calculation; and solution of the Bethe–Salpeter equation to calculate the optical absorption spectrum for the system. Using this absorption spectrum, we have estimated the power conversion efficiency (PCE). Our estimated PCE for this (≈ 1 nm thick) device is $\approx 1\%$, leading to a considerably high power density value. This bilayered heterostructure has not been studied to date in the literature theoretically or experimentally and we have demonstrated its potential application as a Schottky barrier solar cell. Our study predicts that the ZrSe₂(1T)@ZrTe₂(1T) bilayered heterostructure is a suitable material for an ultrathin Schottky barrier solar cell.



[Zn-phenanthroline-dicarboxylate complex: A dual inhibitor of COX-2 and 5-LOX enzymes](#)
D Rambabu, S Sharma, Mayank, N Singh... - ChemistrySelect, 2024

76.

Abstract: A series of new phenanthroline-based metal complexes, coordination polymers are synthesized using 1,10-phenanthroline 2,9-dicarboxylate (PDA) and different metal salts including tin (R-1 to R-3), manganese (R-4), ruthenium (R-5), and zinc (R-6) respectively. The inhibitory activities of synthesized coordination compounds are evaluated towards COX-2 (cyclooxygenase-2) and 5-LOX (5-lipoxygenase) enzymes. Among all the metal-organic coordination complexes, Zn-PDA (R-6) shows most prominent inhibitory activity than other systems with the IC₅₀ value of 0.0524 $\mu\text{g/mL}$ and 0.834 $\mu\text{g/mL}$ for both COX-2 and 5-LOX enzymes, respectively. The synthesized systems were also evaluated for their activity against COX-1 and standard COX-2 inhibitors viz. Rofecoxib and Aspirin. The rationale for R-6 being the most potent metal complex for dual COX-2 and 5-LOX inhibition is demonstrated using docking studies.

Disclaimer: This publication digest may not contain all the papers published. Library has compiled the publication data as per the alerts received from Scopus and Google Scholar for the affiliation “Indian Institute of Technology Ropar” for the month of June, 2024. The author(s) are requested to share their missing paper(s) details if any, for the inclusion in the next publication digest.